



NRC Publications Archive Archives des publications du CNRC

Intracrystalline Sorption of Water and Organic Substances in Tetracalcium Aluminate Hydrate

Dosch, W.

For the publisher's version, please access the DOI link below./ Pour consulter la version de l'éditeur, utilisez le lien DOI ci-dessous.

Publisher's version / Version de l'éditeur:

<https://doi.org/10.4224/20331487>

Technical Translation (National Research Council of Canada), 1971

NRC Publications Record / Notice d'Archives des publications de CNRC:

<https://nrc-publications.canada.ca/eng/view/object/?id=22fdc693-d8d6-4b42-99fd-4987566fa86c>

<https://publications-cnrc.canada.ca/fra/voir/objet/?id=22fdc693-d8d6-4b42-99fd-4987566fa86c>

Access and use of this website and the material on it are subject to the Terms and Conditions set forth at

<https://nrc-publications.canada.ca/eng/copyright>

READ THESE TERMS AND CONDITIONS CAREFULLY BEFORE USING THIS WEBSITE.

L'accès à ce site Web et l'utilisation de son contenu sont assujettis aux conditions présentées dans le site

<https://publications-cnrc.canada.ca/fra/droits>

LISEZ CES CONDITIONS ATTENTIVEMENT AVANT D'UTILISER CE SITE WEB.

Questions? Contact the NRC Publications Archive team at

PublicationsArchive-ArchivesPublications@nrc-cnrc.gc.ca. If you wish to email the authors directly, please see the first page of the publication for their contact information.

Vous avez des questions? Nous pouvons vous aider. Pour communiquer directement avec un auteur, consultez la première page de la revue dans laquelle son article a été publié afin de trouver ses coordonnées. Si vous n'arrivez pas à les repérer, communiquez avec nous à PublicationsArchive-ArchivesPublications@nrc-cnrc.gc.ca.



PREFACE

Researchers in cement chemistry have recently become aware that many of the problems associated with the dimensional stability of concrete are due to the fact that the great majority of the hydration products of cement, which include tetracalcium aluminate hydrate, are made up of layered crystals.

A great variety of organic compounds are now being used as admixtures to improve certain properties of cements. This paper describes how these organic compounds react and form complexes by attaching themselves between the layers of tetracalcium aluminate hydrate, and how this results in swelling.

The Division is grateful to Mr. D. A. Sinclair of the Translations Section, National Research Council, for translating this paper and to R. F. Feldman of this Division who checked the translation.

Ottawa
October 1971

N. B. Hutcheon
Director

NATIONAL RESEARCH COUNCIL OF CANADA

Technical Translation 1491

Title: The intracrystalline sorption of water and organic substances in tetracalcium aluminate hydrate

(Die innerkristalline Sorption von Wasser und organischen Substanzen an Tetracalcium-aluminathydrat)

Author: W. Dosch

Reference: Neues Jahrbuch für Mineralogie, 106 (2): 200-239, 1967

Translator: D. A. Sinclair, Translations Section, National Science Library

THE INTRACRYSTALLINE SORPTION OF WATER AND
ORGANIC SUBSTANCES IN TETRACALCIUM ALUMINATE HYDRATE

Abstract

Tetracalcium aluminate hydrates are known as hydration products of cement. The true cell is uncertain, but for the pseudocell, including the arrangement of interlayer water a model is given being in good agreement with the x-ray data of the five hydration stages. Tetracalcium aluminate hydrates are the first example for layer structured crystals containing neutral sheets, which are highly capable of interlayer sorption of water and neutral organic compounds. Sorption complexes with approximately 500 selected organic substances have been investigated. Basal reflexes, their position indicating the arrangement of sorbed molecules, are generally sharp. Regarding the complexes with alcohols, the possible configuration and bonding conditions between organics and inorganic matrix are extensively discussed. A survey on numerous homologous organic substances shows the reactivity of tetracalcium aluminate hydrate. Besides complexes with Van der Waals or H bonding there are also homopolar bonded interlayer complexes. It is also possible to imbed a mixture of two or more organic compounds. Another variant is the imbedding of water mixed with organic compounds. The de- and rehydration reactions of these products in the range from -20 to +100°C have been studied.

1. Introduction

The unidimensional interlamellar sorption of organic molecules on inorganic layer lattices is a familiar phenomenon to clay specialists. Since its discovery, a voluminous literature has appeared on the organic compounds of clay, which Nahin⁽¹⁾ described as "hybrid unions of organic and inorganic materials". Comprehensive treatments of this subject will be found in the books of Iler⁽²⁾, Hauser⁽³⁾, Grim⁽⁴⁾ and Jasmund⁽⁵⁾, and in papers by McEwan⁽⁶⁾, Jordan⁽⁷⁾, Nahin⁽¹⁾ and Weiss^(8,9). For the state of

research at a given time one may consult the technical press and the North American "Symposia on Clay-Organic Complexes", which are held during the annual National Conferences and are published in "Clays and Clay Minerals Proceedings".

The substance in which Hofmann and Frenzel⁽¹⁰⁾ observed the phenomenon of unidimensional intracrystalline swelling for the first time in 1930 was not a clay mineral but graphitic acid. With increasing knowledge about the organic compounds of clay, interest also increased in the study of interlamellar sorption in layer crystals with structures different from those of the clay minerals. As Table I (after McEwan⁽⁶⁾) shows, this question has also been broached many times. The Table could be expanded by further contributions of Weiss, who is a leader in this field, on the swelling of dititanates⁽¹¹⁾ and polyphosphates⁽¹²⁾.

A common characteristic of these different swelling compounds is their construction from macroions which are bound by interchangeable gegenions.* In general, the macroions (anions or cations) have a layer structure, but in the case of polyphosphates, exceptionally, they form chains. The mechanism of interlamellar sorption and the choice of molecules capable of embedment depends strongly on the charge density of the layers or chains and the type and state of hydration of the gegenions^(13,14,15). The gegenions may have a stronger influence on the course of the intracrystalline swelling than the chemical composition of the sheets or chains themselves. This applies not only to the mentioned inorganic swelling substances, but also to such biological products as collagen^(16,17) or desoxyribonucleic acid (DNA)⁽¹³⁾, in which ammonium, guanidinium and carboxylate ions of the collagen amino acids or phosphate ions of DNA can be saturated.

It is therefore interesting to note that this large group of substances, whose intracrystalline swelling can be controlled by or may even be caused by ion processes, can also be compared to electroneutral lattices with swelling capacity. These include

* i.e., an ion with a charge opposite to the charge of the surface at which it is sorbed.

the complex cyanides of the transition metals, studied by Weiss⁽¹³⁾. In these compounds, the consumption of neutral polar molecules on swelling appears to be due to the tendency of the transition metals to undergo a change from 4-coordination to 6-coordination.

The swelling capacity of tetracalcium aluminate hydrate, which is the subject of the present paper and which is also made up of neutral sheets, takes a greater variety of forms than that of the complex cyanides.

The great majority of the hydration products of cement, which include tetracalcium aluminate hydrate, constitute layer crystals. Previously, nothing was known about the intracrystalline sorption of organic compounds by the products of cement hydration even though cements had been treated with a large number of organic substances, sometimes in order to determine the corrosiveness of these substances, sometimes as admixtures to improve certain properties of the cements (cf. ^(18,19)). In the present paper, we shall describe the unidimensional, intracrystalline swelling of tetracalcium aluminate hydrate with water and organic compounds.

The author has so far produced about 500 different sorption complexes of tetracalcium aluminate hydrate. It will be possible to discuss only a few of these briefly here. These have been chosen so as to provide as complete a picture as possible of the reactivity of tetracalcium aluminate hydrate. Before taking up the reactions with organic substances, we deal with the various hydrate stages of tetracalcium aluminate hydrate and, as far as possible, its structure. The possible configuration and binding conditions of complexes with organic substances are then discussed, using the monovalent alcohols as an example. The sorption complexes in which one or more organic molecules take part are taken up one by one. Another classification is given by the fact that the organic components are linked to the inorganic host lattice normally by Van der Waal's forces or H binding, but sometimes also in homopolar arrangement. Finally, rehydration and dehydration processes with sorption complexes are dealt with.

2. Experimental Part

(a) Preparation of tetracalcium aluminate hydrate: For the preparation of adequate quantities of uniformly constituted initial product, a solution of sodium aluminate which was free of CaO and CaO₂ was converted by the method described by zur Strassen and Dosch⁽²⁰⁾.

(b) The organic reagents were obtained from Fluka AG, Buchs, Switzerland. Samples marked "purissimum" were used directly. Those marked "technicum", and in cases of doubt those marked "purum" also, were further purified by distillation or recrystallization.

(c) Preparation of organic complexes: If the organic substances are liquid at room temperature, suspensions were made with tetracalcium aluminate hydrate, generally in the hydrate stage $4 \text{ CaO} \cdot \text{Al}_2\text{O}_3 \cdot 11 \text{ H}_2\text{O}$. Powder preparations for x-ray analysis, textured to a large extent with respect to 001, were produced by coating slides with the filtered crystals. Solid organic substances were dissolved in ether, acetone or acetonitrile, which do not themselves react at all with tetracalcium aluminate hydrate, or do so only very slowly. In a few specially noted cases, water or benzene was used as the solvent.

(d) X-ray methods:

(α) Since pure tetracalcium aluminate hydrates are extremely sensitive to atmospheric CO₂, the x-ray "climate-control chamber" developed by Dosch⁽²¹⁾ (Figure 1a) was used to hold the powder. After the chamber is brought to the correct temperature, the preparation was loaded into it in a "glove box". At the bottom is a small dish containing air-conditioning agents with which desired water vapour partial pressures or organic vapour atmospheres can be produced.

(β) For the study of moist preparations, filter paper was cemented into the depression in the circular microscope stage, as shown in Figure 1c. The projecting

strip of paper is dipped into the dish containing the solvent and acts as a wick.

(γ) X-ray pictures of suspensions were made in a specially designed compartment⁽²²⁾ shown in Figure 1b. This compartment can also be temperature-controlled. The suspension is stirred.

3. Tetracalcium Aluminate Hydrates, Stages of Hydration and Construction of the Pseudocell

There are at least five different hydrates of the general composition $4 \text{ CaO} \cdot \text{Al}_2\text{O}_3 \cdot \text{water}$. They constitute hexagonal or pseudohexagonal layer crystals, from the structure of which a number of quaternary compounds may also be derived, e.g., with CO_2 or SO_3 ⁽²³⁾. Thus the tetracalcium aluminate hydrates are easily converted into carbonate hydrates simply by the carbon dioxide in the air. The similarity of the latter to the compounds that are free of CO_2 has led to a number of contradictions and confusions in the literature.

Zur Strassen and Dosch⁽²⁰⁾ studied the relationship between the individual tetracalcium aluminate hydrates and the tetracalcium aluminate carbonate hydrates. The hydrates were characterized by water content and very long basal reflections (Figure 2). The five ternary hydrates have basal spacings of 10.6, 8.2, 7.9, 7.4 and 7.2 Å corresponding to hydrate stages with 19, 13, 12, 11 and 7 $\text{H}_2\text{O}/4 \text{ CaO} \cdot \text{Al}_2\text{O}_3$. From the compound $3 \text{ CaO} \cdot \text{Al}_2\text{O}_3 \cdot \text{CaCO}_3 \cdot \text{water}$ we get two hydrates with $d_{001} = 7.6 \text{ Å}$, 11 H_2O and $d_{001} = 7.15 \text{ Å}$, 6 H_2O . The "quarter carbonates" are poorer in CO_2 ($3 \text{ CaO} \cdot \text{Al}_2\text{O}_3 \cdot 3/4 \text{ CaO} \cdot 1/4 \text{ CaCO}_3 \cdot \text{water}$ with $d_{001} = 8.2 \text{ Å}$, 12 H_2O and $d_{001} = 7.7 \text{ Å}$, 9 H_2O). Quarter carbonate hydrate has the same composition as the mineral, hydrocalumite, the basal spacing of which (only a 12 hydrate is known) is, however, 7.9 Å. Quarter carbonate hydrate (8.2 Å) and $4 \text{ CaO} \cdot \text{Al}_2\text{O}_3 \cdot 13 \text{ H}_2\text{O}$ have the same basal spacing and are therefore easily confused. However, these compounds can be distinguished radiographically through a

dehydration process. Roberts⁽²⁴⁾ two polymorphous modifications α and β - $4 \text{ CaO} \cdot \text{Al}_2\text{O}_3 \cdot 13 \text{ H}_2\text{O}$ ($d_{001} = 8.2$ and 7.9 \AA respectively) are actually two different hydrates with 13 and 12 H_2O respectively.

In the present study, CO_2 was carefully excluded by means of a glove box and the climate-controlled x-ray chamber. Therefore, only the ternary hydrates occur, see Figure 2, right hand column.

The structure of tetracalcium aluminate hydrate, hereinafter abbreviated to C_4AH_x^* , has not been clarified. It has been investigated by Brandenberger⁽²⁵⁾, Tilley, Megaw and Hey⁽²⁶⁾, Buttler, Dent Glasser and Taylor⁽²⁷⁾ and Grudemo⁽²⁸⁾. Common to all attempts at interpretation is the assumption of a layer structure and hydroxyl binding of the total oxygen in the structural element $\text{Ca}_2\text{Al}(\text{OH})_7$ of the C_4AH_7 compound containing no water of crystallization. Composition and sequence of individual layers have been variously interpreted. Brandenberger, Tilley et al. and Grudemo all postulate different two-sheet arrangements for the pseudocell, but none of these is directly compatible in its geometry with the measured lattice constants, nor adequately explains the crystal-chemical behaviour of the C_4A hydrates.

Buttler, Dent Glasser and Taylor have shown that the pseudocell contains only one sheet of octahedrons and has a structure similar to that of portlandite, $\text{Ca}(\text{OH})_2$. Imagine one in a portlandite sheet replaced by Al^{3+} from 3 Ca^{2+} positions, Figure 3a. The charge of the octahedral sheet is not yet balanced; the seventh OH ion of the structural element $[\text{Ca}_2\text{Al}(\text{OH})_6]\text{OH}$, hereinafter called "outer OH", is present in the OH octahedron vacancies over the Al positions, Figure 3b.

The real cell, which is complicated by different insertion arrangements of the structural element, is unknown. For the following considerations it is sufficient to know the shape of the pseudocell. Similarly, the basal reflection indexing here applies only to the pseudocell. The unidimensional swelling || c

* Abbreviated nomenclature: C = CaO ; A = Al_2O_3 ; H = H_2O .

is correctly described by these data. The 001 indices of the true cell may be three times or more greater than those of the pseudocell, cf. Kuzel⁽²⁹⁾.

From the data of Buttler et al. it appears that the outer OH's occupy only one side of the octahedron layer. The basal spacing of the compound C_4AH_7 , without water of crystallization was determined by thermal dehydration to be 5.8 to 6.5 Å (wide reflections). However, at the dehydration temperature of 122°C the lattice was attacked. Lines of $Ca(OH)_2$ appeared in the x-ray diagram of C_4AH_7 .

Zur Strassen and Dosch got sharply crystallized C_4AH_7 with $d_{001} = 7.2$ Å at room temperature in the x-ray climate-control chamber via P_2O_5 , (cf. Figure 2). This value for the dehydration at room temperature is preferred to the result of the thermal dehydration; it is compatible only with a configuration in which the outside OH groups are disposed on both sides of the octahedron sheet or are distributed statistically, Figure 3b. It is assumed that the outside OH groups are extremely polarized relative to the Al^{3+} and penetrate very deeply into the sheet of octahedral hydroxyl ions.

On the basis of this model of the octahedron sheet with two differently arranged types of OH groups, we can construct a plan of the possible structure of the hydrate stages of C_4AH_x , Figure 4. Accordingly, octahedron sheets are piled up in C_4AH_7 in such a way that the outside OH groups lie vertically one above the other. (A discrete arrangement of the outside OH groups of two sheets relative to each other is required only for this hydrate.) This is possible because a tetrahedral charge distribution may be expected for the extremely polarized hydroxyl ions which permits hydroxyl binding, similar to that found by Bernal and Megaw⁽³⁰⁾ for the series of layers in hydrargillite. Water of crystallization is acquired, according to Figure 4, in such a way that fully occupied interlayers are formed, with or without participation of the outside OH groups for all stages of hydration. In the segment of the octahedron sheet being observed (2 "molecules" of $4 CaO \cdot Al_2O_3 \cdot$ water as in Figure 3), a maximum of 12 OH^- or H_2O can be accommodated.

In C_4AH_{11} , this interlayer comprises 4 outside OH + 8 H_2O = 12; compared with the substance free of water of crystallization, the basal spacing increases by only 0.2 Å, since the layer in C_4AH_7 already expanded by outside OH is substantially filled only by the acquisition of water. For C_4AH_{13} , a fully occupied layer of 12 H_2O is obtained without participation of the outside OH. In C_4AH_{19} , there are two fully occupied layers of water. C_4AH_{12} cannot be fitted directly into this scheme. Possibly layers of the 11 and 13 hydrate are present in this hydrate one above the other in irregular alternation. A shift of the 7.9 Å reflection from 12 hydrate in the direction 8.2 Å or 7.4 Å (13 and 11 hydrate respectively) was not, to be sure, observed.

4. Complexes with Monovalent Alcohols

The complexes of the primary alcohols $C_nH_{2n+1} \cdot OH$ with C_4AH_x give sharply defined basal reflections which shift with increasing numbers of carbon atoms in homologous alcohols towards smaller glancing angles, Table II. The incorporation rate decreases with increasing C number of the alcohols. Alcohols C_{11} to C_{20} (dissolved in ether or acetone) are no longer acquired at room temperature.

Alcohols with branched chains are sorbed much less rapidly than their straight-chain isomers. In complexes of the branched-chain alcohols, the basal spacings in general do not increase with increasing C number. Constant values of $d_{001} \sim 10.7$ Å are obtained, cf. Figure 5a, b. It will be seen below that this spacing is characteristic of organic molecules where the carbon chains are disposed parallel to the inorganic layers. The straight-chain alcohols show a steep angle relative to the inorganic layer.

The complex with i-amyl alcohol, Figure 5b, shows a second, less intense series of 001 reflections with $d_{001} = 20.8$ Å. This value lies between the branches of the normal alcohols C_4 (20.2 Å) and C_5 (22.0 Å), Figure 5c, Table II. The isoalcohol can be sorbed not only in a flat sheet, but also in an oblique sheet arrangement. In the latter case, the V-shaped branch of the CH_3 groups in end

position exactly explains the position of the i-alcohol between the neighboring n-alcohols.

For measurement of a short-chain alcohol, the climate-controlled x-ray chamber was used in combination with the wick stage, Figure 1c, Figure 6. The dry filter paper plate of the stage was coated with C_4AH_{12} ($d_{001} = 7.9 \text{ \AA}$) and the wick was allowed to extend into the first empty dish on the floor of the chamber. After x-raying the first two basal reflections of the 7.9 \AA hydrate, the goniometer was set and locked at the angle 3.42° $\theta \cong 12.9 \text{ \AA}$ of the 001 reflection of methanol- C_4AH_x . After opening the thermometer tube, the dish was filled with methanol from a pipette. The ascent of the alcohol up the wick and into the preparation could be observed through the inspection window. The intensity of the adjusted reflection increases simultaneously with the start of wetting, and reaches its maximum after a few seconds, cf. time scale. The record on the left in Figure 6 was then made. The formation of the methanol complex was quantitative.

Similar tests with alcohols of higher C number were made with the aid of the suspension chamber, Figure 1b. Up to n-butanol (C_4) the alcohol complexes form within a few minutes. Between C_5 and C_{10} (inclusive) the sorption rates are much slower - 10 to 20 hours.

Postulated configurations of the complexes:

Figure 7 shows the change of basal spacing as a function of the C number for the C_4AH_x complexes of the standard alcohols C_1 to C_{10} . The points on the slightly zigzag curve lie on two parallel straight lines. The upper dashed line applies to alcohol complexes with C_{even} , and the lower one for C_{odd} , cf. differences of basal spacing, Table II. Alcohols C_9 and C_{10} depart from exact linearity in the direction of somewhat higher basal values.

In the linear region, for the complexes with alcohols C_1 to C_8 , the mean increase of basal spacing for two homologous alcohols is given by $\Delta d_{001}/\Delta n = 16.38/7 = 2.34 \text{ \AA}/C \text{ atom}$. On the longitudinal axis of a zig-zag carbon chain the C - C distance is 1.27 \AA .

Since this distance is much smaller than the experimental value of 2.34 \AA , it must be assumed that in each case two alcohol molecules are situated one behind the other and make a certain angle with the inorganic layer. The sine of the angle of inclination is $\sin \phi = 2.34/2 \cdot 1.27$; $\phi \sim 67^\circ$. For various reasons, this angle cannot be stated with greater accuracy. Since the measured d values can be assigned to two parallel straight lines, the slope of which determines the angle of inclination, the ϕ holds, within the accuracy of determination, for alcohols with both C_{even} and C_{odd} .

In the x-ray diagrams, the intensities of the odd orders of the 001 reflections are increased, those of the even orders decreased, cf. Figure 5c. (In the flat-sheet complexes of the isomeric alcohols with $d_{001} \sim 10.7 \text{ \AA}$, the 001 intensities decrease continuously with increasing glancing angle, corresponding to the dependence of the polarization factor, Figure 5a, b). The same sequence of intensities is known from the crystallized pure alcohols, fatty acids, etc. As Prins⁽³¹⁾ has shown, this is due to the intensity distribution of long molecules which are situated "head-to-head", "foot-to-foot", Figure 8. Accordingly, we must picture the configuration of the alcohol/ C_4AH_x complexes as having "foot-to-foot"-situated alcohol which make an angle of 67° , adhering with their OH groups to two oppositely situated C_4AH_x sheets in each case. After we recognize this general principle of arrangement, the data of Table III can be used to draw further conclusions about the possible construction of the complexes.

Figure 9a shows carbon double chains erected between inorganic layers (hatched). For the present, the character of the binding between alcohol-OH and the inorganic layer is left out of account. In chains with C_{even} , the outermost member of the chain, oxygen, stands at a steep angle ($1.43 \cdot \cos 58^\circ = 0.76 \text{ \AA}$), while in those with C_{odd} , it is at a flat angle ($1.43 \cdot \cos 12^\circ = 1.40 \text{ \AA}$) relative to the C_4AH_x sheet. The sequence $0.8..1.4..0.8..(\text{\AA})$ for the transition from an alcohol to its next homolog corresponds exactly to the observed values. This is obtained from the zigzag form of the chains and the angle of inclination ϕ .

However, since the rather large change of $2 \cdot 1.40 \text{ \AA}$ was measured for the transition of the alcohol complexes C_{odd} to C_{even} , the zigzag planes still have to be rotated 180° about the axis of inclination, as is evident from Figure 9b. The sequence and absolute amounts of the observed basal value changes are in agreement with this arrangement.

The distance indicated in Figure 9 of about 3.5 \AA between two oppositely situated CH_3 groups was taken from numerous structure data for pure crystallized organic compounds^(31,36). Because of the angle of inclination, we get two different intermolecular distances with this value, namely 3.5 and $2.8 \text{ \AA} \parallel c$ depending on the arrangement of the chain molecules in Figure 9a or b.

Since the oxygen atoms of the alcohols make two different angles with the C_4AH_x layer, we cannot simply postulate a directed binding, say H bridges. An undirected binding, Van der Waals contact, cannot, on the other hand, explain the relative stability of the alcohol- C_4AH_x complexes.

Models with H binding are shown in Figure 9c. An H binding is best if the components $\text{O} - \text{H} \cdots \text{O}$ are linearly directed, cf. Luck⁽³²⁾. (The case of cyclic H binding, which is less favourable from the energy standpoint, is not discussed here.)

The H bridges, Figure 9c, alternately make angles of 58 and 12° with the normals of the C_4AH_x sheets. The increase of basal values is $1.9..0.3..1.9..(\text{\AA})$, contradictory to the experimental result. If, in the transition from one alcohol to the next, the zigzag planes are rotated each time 180° about the axis of inclination, Figure 8d, then, while the angle of the H bridges always remains the same, the basal increase from one alcohol to the next is now a uniform 1.2 \AA . However, this cannot be right either.

We therefore return to the concepts of the C_4AH_x lattice structure, Figure 3. The outer OH groups which neutralize a complete residual charge of Al^{3+} are extremely polarized. Al^{3+} is surrounded symmetrically by 6 Ca^{2+} . The polarization of the outside OH groups is therefore almost solely determined by the Al^{3+} located rather loosely in its octahedral position, situated

directly below (or above) the OH. In hydrargillite, the polarizing effect of Al^{3+} is thought to impose a charge distribution with tetrahedral symmetry on the OH groups⁽³⁰⁾. In the C_4AH_x structure, this distortion of the electron shell of the outside OH ion continues to exist, so that an angle of 58° to the normal of the inorganic layer ($\sim 1/2$ tetrahedron angle) seems not improbable for the start of H binding.

The hydroxyl ions of the octahedron layer, on the other hand, are surrounded by 2 Ca^{2+} and 1 Al^{3+} . As may be concluded from a comparison of hydrargillite and portland lattices, their polarization ought to be weaker than that required for the outside OH. The polarization vector originating at Al^{3+} will prevail over the influence of the Ca^{2+} , and also in the case where a tetrahedral charge distribution in the OH is attained, the proton of which is shifted a small angle away from the normal.

On the assumption that this angle is about 12° and that the alcohols with C_{even} form H bridges with the octahedral OH ions, while those with C_{odd} form H bridges with the outside OH groups at an angle of 58° , we get the arrangement according to Figure 10. This shows the various positions and the polarization vectors of octahedral and outside OH. Calculation with the experimental basal spacings shows a difference of height of 0.7 \AA for the two kinds of OH groups.

For the distance between the centres of two oppositely situated OH ions in the octahedral layer we get $3.1 \pm 0.2 \text{ \AA}$; two outside OH groups are situated in planes that are $4.5 \pm 0.2 \text{ \AA}$ apart. The latter value can be used to verify the construction of the compound C_4AH_7 ($d_{001} = 7.2 \text{ \AA}$) without water of crystallization. It is assumed here that the outside OH groups of two sheets are disposed, as already stated, vertically one above the other, and are linked by hydroxyl binding (Figure 4). The intermolecular spacing $\text{O}^{\text{H}}_{\text{H}}\text{O}$, according to Evans⁽³³⁾, is 2.7 \AA ; $4.5 + 2.7 = 7.2 \text{ \AA} = c$ value of the pseudocell of C_4AH_7 .

The model deduced for the alcohol complexes with H binding correctly reflects the observed differences of basal spacings for successive alcohols and the absolute values of the basal spacings.

To assume that the alcoholic hydroxyl groups must be linked to OH groups of the inorganic layer that differ from each other in respect to arrangement and state of polarization appears at first glance to be stretching matters somewhat; however, in the explanation to Figure 9 we showed that for binding to equivalent inorganic OH groups we get uniform basal increases with increasing C number, and the alcohols opposite the CH₃ groups in end position must then take on two different arrangements in relation to the axis of inclination for C_{even} and C_{odd} respectively. The first is incompatible with the measured basal increases, the second is improbable. The angle of inclination, which must be approximately equal for C_{even} and C_{odd} (Figure 7), is determined by the packing arrangement of parallel alcohol molecules. Brindley and Moll⁽³⁵⁾, following the lead of Kitaigorodskii⁽³⁶⁾, considered the shearing of close-packed aliphatic chains in the direction of the chain axis. The discrete shear values are the result of CH₂ spheres dropping into CH₂ sphere vacancies in neighboring chains. Angles of 90°..73.4°..59.1° are obtained between the axis of the chains and the surface on which the chains rest, depending on the amount of shear. The angle of inclination 67° for the alcohol complexes C₁ to C₈ is close to the packing angle 73.4°. If the packing parallel to the chain axis is the same for all* alcohols, it may be expected that the arrangement of the CH₃ groups in end position will not change in relation to the axis of inclination from one homolog to the next without a compelling reason.

Benzyl alcohol, the C₆H₅CH₂ complex of which also gives a sharp x-ray diagram with enhanced odd 001 reflections, is cited in Table II as an example of the aromatic alcohols. This alcohol fits logically into the configuration model, Figure 9.

Emerson⁽³⁴⁾ constructed a model for H binding of alcohols which are disposed with the carbon chains parallel to the inorganic layers for montmorillonite/alcohol complexes. Similar flat sheet arrangements can also be postulated for the C₄H₉ complexes with i-propanol (d₀₀₁ = 10.7 Å) and i-amyl alcohol (d₀₀₁ = 10.6 Å).

* With the exception of n-nonanol and n-decanol, which are incorporated at a steeper angle of inclination.

According to Table II, a total of four different C_4AH_x methanol complexes were found with $d_{001} = 12.9, 14.4, 13.9$ and 10.8 \AA . It is assumed that double methanol sheets are present in the complexes with 12.9 and 14.4 \AA . Of the 10.8 \AA complex it was shown qualitatively that it contains less methanol and probably constitutes a single-sheet arrangement. The 13.8 \AA complex has not yet been clarified.

Montmorillonite Complexes with Monovalent Alcohols

Alcohol complexes of montmorillonite were investigated by Hofmann, Endell and Wilm⁽³⁷⁾, MacEwan⁽³⁸⁾, Barshad⁽³⁹⁾, Glaeser⁽⁴⁰⁾, Greene-Kelley⁽⁴¹⁾, Emerson⁽³⁴⁾, Brindley and Hoffmann⁽⁴²⁾, and Brindley and Ray⁽⁴³⁾. The results, essentially, are as follows. Alcohols C_1 to C_{16} form flat sheet arrangements (basal spacing $13 - 14.5 \text{ \AA}$). The alcohols $C_{1,2,4,6}$ when present in excess can also build up flat double sheets (basal spacing 17 \AA). For complexes of the alcohols C_9 and C_{10} Barshad found basal values of 34.4 and 36.8 \AA respectively, which can only be explained by the presence of steep double chains, as already deduced for C_4AH_x alcohol complexes. Brindley and Ray studied this phenomenon closely and established a total of four different kinds of complex formation: 1. Flat single sheets for alcohols C_2 to C_{18} ($13 - 14 \text{ \AA}$); 2. Flat double sheets for alcohols C_2 to C_6 ($17 - 18 \text{ \AA}$); 3. At temperatures above the melting points of the alcohols C_6 to C_{18} , an arrangement of alcohol double chains at a steep angle in relation to the montmorillonite sheet; 4. At temperatures below the melting point for alcohols C_{10} to C_{18} a similar arrangement to 3, but with still larger basal values. The angle of inclination is 38° (case 3) or 77° (case 4). Brindley and Ray assumed H binding for the contact between the alcoholic hydroxyl and the oxygen of the silicate sheets. The alcohols with C_{odd} were not included in the investigation. Figure 11 shows Brindley's results on Ca montmorillonite in comparison with the alcohol complexes of C_4AH_x . At room temperature, conforming alcohol complexes are formed in the case of C_4AH_x only up to alcohol C_{10} , and for

montmorillonite only starting from alcohol C_{12} (heavy solid curve). The following conclusion may be drawn: for montmorillonite, a steep alcohol double chain probably represents the less favourable special case of incorporation from the standpoint of energy. In the normal case, the alcohol molecules are sorbed in the form of flat single sheets, or in the case of a few short-chain alcohols, also in the form of double sheets.

For the C_4AH_x lattice, however, the steep arrangement is preferred, probably on account of the stronger complex formations; flat sheets are formed only under unfavourable space conditions (secondary or tertiary alcohols) or if the alcohol concentration is too small to construct steep layers.

Alcohol sorption has been chosen as an example, in order to show how the possible configuration and binding conditions of C_4AH_x complexes can be discussed. In what follows, this broader form of representation gives way to a review of various other C_4AH_x complexes, restricting the discussion essentially to the classes of organic compounds which form homologous series.

5. Complexes with Polyvalent Alcohols, Sugars and Hydroxy Acids

Figure 12 shows the basal spacings of the C_4AH_x complexes with the diols $HO-(CH_2)_n-OH$; $n = 2$ to 6 . The trivalent alcohol, glycerine, was also included in this series. The x-ray diagrams show many lines. In addition to the sharp, strong reflections of a 001 series (solid curve), sometimes several 001 series of lower intensity also appear side by side. The complexes were x-rayed after different times (numbers in Figure 12 = days). The complexes showing strong x-ray intensities represent double flat sheets, while some of the lower basal spacings correspond to flat, single sheet arrangements.

Sugar alcohols such as mannitol, sorbitol, etc., a number of mono- and disaccharides, sugar-like substances, such as vitamin C, and

hydroxy acids were converted in the form of saturated aqueous solutions with C_4AH_x . In all cases colloidal solutions developed. Mucilagenous solids were obtained only after adding excess C_4AH_x , but these were amorphous to x-rays. Sorption complexes with sharply defined x-ray diagrams could only be obtained by careful apportioning of the organic compounds. This is demonstrated in Figure 13 on the example of lactose, which is disposed with the plane of its two pyran rings parallel to the C_4AH_x sheets: at the concentration of 0.2 mol lactose/ C_4AH_x the formation of the lactose complex can be recognized only from the weak, broadened reflections ($d_{001} = 14.4 \text{ \AA}$). The main product is C_4A -19-hydrate ($d_{001} = 10.6 \text{ \AA}$). With increasing doses of lactose, the reflections of the 14.4 \AA complex increase and become sharper, while that of the 19-hydrate decreases. Saturation is apparently attained at 1 mol lactose/ C_4AH_x . Further additions of lactose enhance the dispersity; the reflections are weakened, and at 4 mol lactose/ C_4AH_x only about 2% solid substance relative to the initial C_4AH_x could be filtered out.

6. Complexes with Mercaptans

The mercaptans $C_nH_{2n+1}SH$ are related to the alcohols $C_nH_{2n+1}OH$, but differ from them in two properties which must have an interesting effect on the formation of sorption complexes: 1. Unlike the alcohols, the mercaptans are not associated (cf. boiling point!). There is no formation of H bridges, because the electronegativity of sulphur (proportional index 2.5 according to⁽⁴⁴⁾) is much smaller than that of oxygen (3.5). 2. Unlike the alcohols, the mercaptans give an acid reaction.

The formation of complexes with C_4AH_x takes place more quickly than with the alcohols and extends at least up to the mercaptan C_{16} . The thermostability of the complexes with mercaptans is greater than that of alcohols. Figure 14 shows the change in basal spacing with C number. The curve of the 001 series with great intensity (—) makes a straight line, in contrast to the zigzag curve of the alcohol complexes, which is drawn in for comparison (·····).

Among the mercaptan complexes there are two further 001 series with weak intensities (·-·-), approximately parallel to the main curve between C_4 to C_8 . For the complexes of the principal curve it is assumed that the mercaptan molecules form double chains with an angle of inclination of about 40° , up to mercaptan C_8 . The stretched hexadecanthiol molecule (C_{16}) is 24 \AA long. The basal spacing of the corresponding mercaptan complex is only 29.5 \AA . From this it may be concluded that the molecules of the mercaptan C_{16} are arranged "head-to-foot", i.e., their thickness is equal to the length of about one molecule, and they rise steeply between the C_4AH_x sheets. This view is supported by the sorption isotherms, Figure 15: with increasing amounts of octyl mercaptan the reflections of free, C_4AH_x , starting from 4 mol C_8 , vanish; (S) signifies saturation. With mercaptan C_{16} , the point (S) is reached already at 2 mol $C_{16} \cdot SH/C_4AH_x$. [The basal values of the main series of the 001 reflections, of course, are much higher here (31.9 \AA) than in the region of mercaptans supersaturation (29.5 \AA). This dependence of the basal spacing on the concentration of sorbed substance has since been observed in other determinations of the sorption capacity; it is not discussed further here.] In the C_4AH_x lattice, the area of a molecule of $4 \text{ CaO} \cdot \text{Al}_2\text{O}_3 \cdot \text{water}$ is about 56 \AA^2 . An extended alkyl chain, according to Weiss⁽⁹⁾, has a diameter of about 21 \AA^2 . In the "head-to-foot" arrangement (hexadecanthiol) only two molecules of mercaptans are sorbed, but on incorporation of double chains four molecules of mercaptans C_8/C_4AH_x are sorbed.

7. Complexes with Amines

In connection with clay minerals, the sorption complexes of the amines, and especially the amine cations $R \cdot NH_3^+$, have attracted a great deal of attention. According to Jordan⁽⁴⁵⁾, amines C_2 to C_{10} form a flat single sheet while amines C_{12} to C_{18} form flat double sheets. Weiss^(9,46) has produced complexes with alkyl ammonium ions in which the organic chains are disposed in "head-to-foot" arrangement between the silicate layers. The angle of

inclination depends on the length of the alkyl chain and the layer charge. The high binding strength of these substances is due to the fact that the alkyl ammonium ions take over the function of the gegenions which are interchangeable with them, and furthermore are bound by H bonds to the oxygen of the tetrahedron layer.

The neutral layers of C_4AH_x , of course, can sorb only the amine bases $R \cdot NH_2$; the electrostatic binding component disappears here. Figure 16 shows the increase of basal spacing of C_4AH_x /amine complexes with increasing C number. From amine C_3 on, the curve takes a zigzag shape, although not as pronounced a one as that for the monovalent alcohols. The amines form double chains with an angle of inclination close to 90° .

The x-ray diagrams of the C_4AH_x complexes α -, ω -diamines $H_2N-(CH_2)_n-NH_2$ have complex constructions; some of the reflections are widened. The basal spacings can be explained with flat single or double sheet arrangements, and from $n = 5$ on the diamines have steep slopes and adhere each with a NH_2 group to the oppositely situated C_4AH_x sheets.

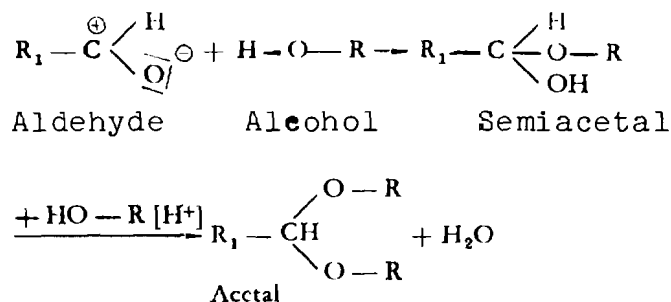
8. The Influence of the Dielectric Constant on the Formation of the Complex

In the case of intercrystalline absorption of organic compounds by montmorillonites, the dielectric constant plays an important part. Substances with high dielectric constants, e.g., nitro-methane⁽⁵⁹⁾ or acetonitrile⁽³⁹⁾, form complex arrangements with three flat sheets⁽³⁸⁾ one above the other. On the other hand, these substances are not sorbed interlamellarly. This behaviour can be ascribed to the differences of electrical field in charged lattices (montmorillonite) and uncharged lattices (C_4AH_x).

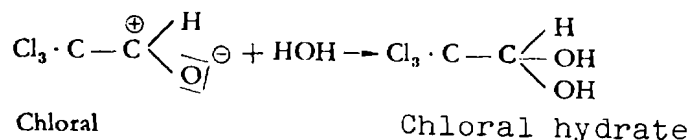
9. Complexes with Aldehydes

With the aldehydes we leave the group of complexes in which only Van der Waals contact or H bridges can be held responsible for

the binding between the inorganic and organic components. For, the addition of aldehydes to C_4AH_x is associated with a strong thermal effect. The chemical reaction that takes place here is not yet clear. It is possible to imagine a process similar to what takes places in the semi-acetals and acetals:



The semi-acetals, however, are instable and the acetals form only under acid catalysis. On the other hand, the reaction



takes place with strong thermal effect, and chloral hydrate is a stable substance ($F = 51.6^\circ$). Other stable aldehyde hydrates are also known. In the C_4AH_x complexes, therefore, we assume a reaction according to the following scheme



which probably leads to homopolar complex formation.

Figure 17 shows the change of basal spacing with C number of the aldehydes in the C_4AH_x complexes. From C_5 on, the x-ray diagrams show two 001 series of different intensities. The aldehyde complexes are thus described by two families of curves, of which the one with the greater basal spacings makes the smaller contribution to the complex formation. Aldehyde C_4 produces only one complex on the curve of lower basal spacings. Aldehyde C_5 forms primarily a complex with $d_{001} = 23.7 \text{ \AA}$, which after two days changes into the 20.0 \AA complex.

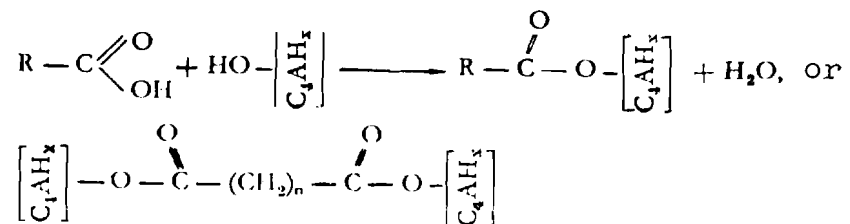
10. Complexes with Carboxylic Acids

If the carboxylic acid is added to a suspension of C_4AH_x in ether cooled to 0°C , a violent reaction takes place, the ether partially evaporates and the product solidifies thixotropically. If we assume that the C_4AH_x lattice is destroyed by this reaction and calcium soaps $(R \cdot COO)_2 \cdot Ca$ are formed, then the product would have to be $8R \cdot COOH/4CaO \cdot Al_2O_3 \cdot \text{water}$. The sorption isotherms, Figure 18, each of which shows a representative of the fatty acids, dicarboxylic acids and phenyl carboxylic acids, make it clear, however, that only four COOH groups are sorbed per mol C_4AH_x (S signifies saturation, disappearance of free C_4AH_x). However, when C_4AH_x /benzene suspensions are titrated with 0.01 n H_2SO_4 or HCl , we get the known compounds of $3 CaO \cdot Al_2O_3 \cdot CaSO_4 \cdot \text{water}$, or $3 CaO \cdot Al_2O_3 \cdot CaCl_2 \cdot \text{water}$ (cf. Chapter 3), in which there is one SO_4^{2-} or 2 Cl^- per one C_4AH_x . The latter case signifies the substitution in C_4AH_x of other inorganic anions for the outside OH. In the carboxylic acids, with double the sorption rate of the inorganic acids, the sorption is no longer determined (solely) by the available outside OH, but also by the area occupied by the organic molecules and their orientation relative to the C_4AH_x layers. According to what has already been stated in connection with the mercaptans, the C_4AH_x lattice can sorb four organic molecules/ C_4AH_x "molecule" in the case of a steeply sloped sheet, but only half of this quantity in the case of a single sheet of steeply sloped organic molecules. The former applies also to the reactions with

$R \cdot \text{COOH}$ (fatty and phenyl carboxylic acids), and the latter for dicarboxylic acids $\text{HOOC} \cdot (\text{CH}_2)_n \cdot \text{COOH}$.

Figures 19, 20, 21, in which the basal spacings of the complexes are again plotted against the C number of the acids, confirm this assumption. The basal values in Figures 19, 20 (from Figure 19 we shall here consider only the family of broken line curves between the triangles) indicate a steeply sloped double chain of acid molecules. The intensities of the uneven 001 reflections are increased. For the dicarboxylic acids $\text{HOOC} \cdot (\text{CH}_2)_n \cdot \text{COOH}$, however, only one extended acid molecule in each case is at a steep angle between C_4AH_x sheets from $n = 3$ on. As exceptions, the dicarboxylic acids with $n = 1, 2$ form flat single layer arrangements.

It is assumed that the acids react primarily with the basic hydroxyl groups of the C_4AH_x lattice and are bound in homopolar fashion in the complexes. Schematically:



These "esters" have not been successfully saponified with soda lye; this is understandable, since Na and Ca salts of the carboxylic acids C_4AH_x also form complexes with the same basal spacings as in the reaction with the pure acids.

11. Alkylation of Tetracalcium Aluminate Hydrate

The discussion of homopolar binding between organic host lattices and organic sorbates is one of the most attractive and at the same time one of the most controversial areas of clay chemistry. Berger⁽⁴⁷⁾ methylated montmorillonite with diazomethane, Gieseking⁽⁴⁸⁾ converted it with acetyl chloride, Deuel et al.^(49,50) prepared the derivatives of benzoyl, mustard gas, epoxide, ethyl and phenyl, and also "montmorillonite chloride" (via SOCl_2) and Mukerjee⁽⁵¹⁾ prepared palmityl and cetyl montmorillonites. We leave open the question of whether and in which of these reactions homopolar complexes were actually produced, and merely mention here a few of the critics of this view: Jasmund⁽⁵⁾, Brown, Greene-Kelley and Norrish⁽⁵²⁾, Greenland and Russell⁽⁵³⁾, Schwarz and Hennicke⁽⁵⁴⁾.

Corresponding reactions with C_4AH_x have been investigated and can be summarized as follows: epoxides do not appear to react, acid chlorides and thionyl chlorides convert C_4AH_x into Friedel's salt. Diazomethane is converted only with acid OH groups and is therefore ineffective. On the other hand, alkylation of the basic OH groups of C_4AH_x with dimethyl and diethyl sulphate in soda lye were successful. Figure 22 shows the possible construction of methyl and ethyl C_4AH_x compared with the corresponding sorption complexes with methanol and ethanol. The OH groups are shown hatched. Of the four volatile methanol complexes, only the 14.4 Å form is given in the figure. The alkylated C_4AH_x compounds are thermally very stable. From these compounds it is possible to produce sorption complexes with a wide variety of organic substances. The effect of water on the alkyl complexes is dealt with in the discussion of Figure 29.

12. Mixed Incorporation, Complexes with two and three Kinds of Molecules

In Figure 23, the x-ray diagrams of the C_4AH_x complexes of hexyl amine, phenyl butyric acid and 1:1 mixture of these substances

are compared. By themselves, hexyl amine and phenyl butyric acid form, as already reported, arrangements with steeply inclined double chains. The reflections of the binary complex are between those of the homogeneous incorporations. In Figure 24 the C_4AH_x /amines already dealt with are plotted alongside the complexes which are formed in the reaction of 1:1 methanol-amine mixtures with C_4AH_x . The examples of Figures 23 and 24 are explained by the fact that double chains of two molecules, one behind the other, of both organic substances participating in the sorption are present in each of the complexes. Thus, the sequence.. C_4AH_x layer..methanol..amine.. C_4AH_x layer applies to the mixed complex. Mixtures of methanol with the long-chain monovalent alcohol are represented in Figure 25. The mixed complex results in two series of 001 reflections which differ definitely from those of the pure alcohols (--). It is evident that long-chain compounds which in pure form do not penetrate into C_4AH_x lattice can nevertheless be sorbed when mixed with a short-chain substance. The same effect is evident in Figure 24, i.e., in the mixtures of methanol and fatty acids, Figure 19. Even non-polar organic molecules such as n-hexane or substances such as nitro-benzene and the like that do not react otherwise, can be incorporated and mixed with easily sorbed substances. Mixed complexes involving a long-chain and various short-chain aldehydes are represented in Figure 26 and compared with the curve of pure aldehydes (--).

Ternary sorption, i.e., where three organic substances are involved, is a complicated process. Figure 27 shows the processes in C_4AH_x complexes consisting of benzoic acid, benzene, and the fatty acids $C_nH_{2n+1} \cdot COOH$ as variable components with $n = 8$ to 20. The arrows show the direction of changes of individual 001 series in the repetition of the x-ray diagrams. A constant 001 series with $d_{001} \sim 14 \text{ \AA}$ is present in all pictures. While irradiation causes evaporation of the liquid benzene*, the basal spacings of the ternary complexes (upper broken curve) are found at the level of the middle broken curve. Proof that this shrinking of the lattice is due to the escape of benzene is found in the

* even though the tests were carried out in a benzene-saturated atmosphere in the climate-controlled x-ray chamber.

fact that the basal spacings again acquired a higher value when the substances were moistened once more with benzene. The other proof that two different acids participate in the complexes is obtained from the comparison of the complexes with pure fatty acids (thin broken curve). Similar observations can also be made on quaternary complexes of C_4AH_x , benzene, lauric acid and various phenyl carboxylic acids in Figure 27.

13. Rehydration and Dehydration of Tetracalcium

Aluminate Hydrate Complexes

Van Olphen and Deeds⁽⁵⁵⁾ investigated the step-by-step hydration of α -picoline and pyridine bentonites and discovered a series of hydrates for both clay organic compounds.

Many of the C_4AH_x complexes were also systematically pre-treated at various relative humidities, as already described previously, in the form of pastes wetted by the organic sorbate, and then x-rayed in the climate-controlled compartment under the same conditions. The basal spacings of almost all C_4AH_x complexes change to a lesser degree between 0 and 100% relative humidity. It is assumed that the effect of water from sorption complexes is associated in particular with the following processes: 1. Some organic compounds are partially or fully substituted by the water and expelled from the lattice. 2. Neighbouring water molecules sometimes influence the binding of the organic molecules to the hydroxyl layer. 3. At high moisture contents, certain organic molecules are bound to hydrate water molecules, and after evaporation of this water they drop into the sheet of inorganic hydroxyl ions. 4. Water molecules may "wedge" themselves between the organic molecules.

Figure 28 shows x-ray diagrams of the C_4AH_x phenyl acetic acid complex: (a) wet with benzene in a benzene atmosphere; (b) dried over P_2O_5 ; (c) rehydrated at 100% relative humidity. In Figure 29 are shown the x-ray diagrams of methyl alkylated C_4AH_x : (a) over 100% relative humidity; (b) after drying over P_2O_5 ; and

(c) after rehydration over water. The methanol complex of C_4AH_x , unlike the methyl group with homopolar binding, is already destroyed at 100% relative humidity and is converted into the C_4A-19 hydrates.

Figure 30 shows a survey of the behaviour of four different sorption complexes: (a) with hexyl amine (double chain, H binding?); (b) ethylene glycol (flat double sheet arrangement, H binding); (c) butyraldehyde (double chain, homopolar binding component) and azelaic acid $HOOC \cdot (CH_2)_7 \cdot COOH$ (steeply inclined molecules which are linked primarily to two opposite C_4AH_x layers). These complexes were x-rayed between -20 to $+100^\circ C$, once over P_2O_5 , then over 100% relative humidity. The basal spacing of hexyl amine C_4AH_x over 100% relative humidity is greater than over P_2O_5 . The same applies to butyraldehyde, although the effect is less marked. The complexes with loose binding over 100% relative humidity are destroyed at a lower temperature than the complexes with homopolar binding (butyraldehyde, azelaic acid). Over P_2O_5 even the complexes with hexyl amine and ethylene glycol remain stable up to high temperatures. In the amine, the aldehyde, and the acid one curve in each case shows a weak bend suggesting reorientation of the organic molecules. In the case of the glycol over P_2O_5 from 70° on a complex is formed with the extremely low basal spacing of 8.8 \AA (single sheet arrangement), which increases with increasing temperature at the expense of the 13 \AA complex. The significance of the sharp single reflection of azelaic acids/100% relative humidity which possesses no high orders and which deteriorates and widens progressively with increasing temperature, is unclarified.

Acknowledgement

The present study was made possible by material aid from the Deutsche Forschungsgemeinschaft. The author owes profound thanks to the Deutsche Forschungsgemeinschaft as well as to the Director of the Mineralogical Institute, Professor E. Baier, for unwavering support. I wish to thank Professor H. zur Strassen and Mr H. Keller for valuable discussions.

References

- (1) NATHAN, P. G.: Perspectives in applied Organo-Clay Chemistry. — *Clays and Clay Miner.* **10** (1963), 257—271.
- (2) HILL, R. K.: *The Colloid Chemistry of Silica and Silicates.* — Cornell University Press, Ithaca, New York (1955).
- (3) HAUSER, E. A.: *Silicic Science.* — D. van Nostrand, Princeton, N. J. (1955).
- (4) GRIM, R. E.: *Clay Mineralogy.* McGraw-Hill, New York (1953).
- (5) JASMUND, K.: *Die silicatischen Tonminerale.* — Verlag Chemie, Weinheim 1951.
- (6) MACLEWAN, D. M. C.: Interlamellar Reactions of Clays and other Substances. — *Clays and Clay Miner.* **9** (1962), 431—443.
- (7) JORDAN, J. W.: Organophilic Clay-Base Thickeners. — *Clays and Clay Miner.* **10** (1963), 299—308.
- (8) WEISS, A.: Organische Derivate der glimmerartigen Schichtsilikate. — *Angew. Chem.* **2** (1963), 113—122.
- (9) — Mica-type layer silicates with alkylammonium ions. — *Clays and Clay Miner.* **10** (1963), 191—234.
- (10) HOFMANN, U. & FRENZEL, A.: Quellung von Graphit und die Bildung von Graphitsäure. — *Chem. Ber.* **63** (1930), 1248—1261.
- (11) WEISS, ALARICH & WEISS, ARMIN: Dilitanate, innerkristallin quellungsfähige Verbindungen. — *Angew. Chem.* **12** (1960), 413—415.
- (12) WEISS, A. & MICHEL, E.: Über Kationenaustausch und innerkristallines Quellungsvermögen bei kettenförmigen Polyphosphaten. — *Z. anorg. allg. Chem.* **296** (1958), 313—332. — Über eine eindimensionale, innerkristalline Quellung bei Mono-n-alkylammonium-polyphosphaten. — *Z. anorg. allg. Chem.* **306** (1960), 277—290.
- (13) WEISS, A.: Die innerkristalline Quellung als allgemeines Modell für Quellungs Vorgänge. — *Chem. Ber.* **91** (1958), 487—502.
- (14) FOSTER, M. D.: The Relation between Composition and Swelling in Clays. — *Clays and Clay Miner.* **3** (1955), 205—220.
- (15) MÉRINO, J.: On the Hydration of Montmorillonite. — *Trans. Faraday Soc.* **42B** (1946), 205—219.
- (16) NEMETSCHKE, TH. & GANSLER, H.: Quellung von Kollagen; Reaktionen mit anorganischen und organischen Kationen. — *Z. Naturforsch.* **16b** (1961), 496—509.
- (17) HOFMANN, U.: Der Verlauf der Quellung bei Kollagen, Schichtsilikaten, Polyphosphaten und Nukleinsäuren. — *Kolloid-Z.* **169** (1960), 58—70.
- (18) BICZOK, I.: *Betonkorrosion-Betonschutz.* — Berlin 1960.
- (19) LEA, F. M.: *The Chemistry of Cement and Concrete.* — Edward Arnold LTD, London (1956).
- (20) ZUR STRASSEN, H. & DOSCH, W.: Untersuchung von Tetracalciumaluminathydraten. I. Die verschiedenen Hydratstufen und der Einfluß von Kohlensäure. — *Zement-Kalk-Gips* **5** (1965), 233—237.
- (21) DOSCH, W.: Röntgen-Feinstrukturuntersuchung luftempfindlicher Pulverpräparate. — *Zement-Kalk-Gips* **5** (1965), 226—232.
- (22) — Untersuchung von Tetracalciumaluminathydraten. II. Beeinflussungen der Quellfähigkeit. — Noch nicht veröffentlicht.
- (23) JONES, F. E.: Hydration of calcium aluminates and ferrites. — *Chemistry of Cement, Proc. Fourth Internat. Symposium, Washington 1960*, 205—242.
- (24) ROBERTS, M. H.: New Calcium Aluminate Hydrates. — *J. appl. Chem.* **7** (1957), 543—546.
- (25) BRANDENBERGER, E.: Kristallstrukturelle Untersuchung an Ca-Aluminathydraten. — *Schweiz. min. petrogr. Mitt.* **13** (1933), 569—570.
- (26) TILLEY, C. E.; MEGAW, H. D. & HEY, M. H.: Hydrocalumite ($4\text{CaO} \cdot \text{Al}_2\text{O}_3 \cdot 12\text{H}_2\text{O}$) a new Mineral from Sawt Hill, Co. Antrim. — *Miner. Mag.* **23** (1943), 607—615.
- (27) BUTLER, F. G.; DENT GLASSER, L. S. & TAYLOR, H. F. W.: Studies on $4\text{CaO} \cdot \text{Al}_2\text{O}_3 \cdot 13\text{H}_2\text{O}$ and the Related Natural Mineral Hydrocalumite. — *J. Amer. Ceram. Soc.* **42** (1959), 121—126.
- (28) GUEDIMIO, A.: The Microstructure of Hardened Cement Paste. — *Chemistry of Cement, Proc. Fourth Internat. Symposium, Washington 1960*, 615—647.
- (29) KUZEL, H.-J.: Synthese und Röntgenuntersuchung des $3\text{CaO} \cdot \text{Al}_2\text{O}_3 \cdot \text{CaSO}_4 \cdot 12\text{H}_2\text{O}$. — *N. Jb. Miner. Mh.* **7** (1965), 193—197.

- (30) BERNAL, J. D. & MEGAW, H. D.: The function of hydrogen in intermolecular forces. I. The hydroxylbond. — *Proc. roy. Soc. London* (1935) 151, 384—420.
- (31) BIJVOET, J. M.; KOLKMEIJER, N. H. & MACGILLAVRY, C. H.: Röntgenanalyse von Kristallen. — Berlin (1940), 174—175.
- (32) LUCK, W.: Zur „Stereochemie“ der Wasserstoffbrückenbindung. — *Naturwiss.* 52 (1965) 3—31; 49—52.
- (33) EVANS, R. C.: Einführung in die Kristallchemie. — J. A. Barth, Leipzig 1954.
- (34) EMERSON, W. W.: Organo-clay complexes. — *Nature* 180 (1957), 48—49.
- (35) BRINDLEY, G. W. & MOLL, W. F.: Complexes of natural and synthetic Ca-Montmorillonites with fatty acids (Clay-organic Studies-IX). — *Amer. Miner.* 50 (1965), 1355—1370.
- (36) KITAIGORODSKII, A. I.: Organic Chemical Crystallography. — Consultants Bureau, New York, with revisions (1961).
- (37) HOFMANN, U.; ENDELL, K. & WILM, D.: Röntgenographische und kolloidchemische Untersuchung über Ton. — *Angew. Chem.* 47 (1934), 539—547.
- (38) MACEWAN, D. M. C.: Complexes of Clays with organic Compounds. I. Complex Formation between Montmorillonite and Halloysite and certain Organic Liquids. — *Trans. Faraday Soc.* 44 (1948), 349—367.
- (39) BARSHAD, I.: Factors affecting the interlayer expansion of vermiculite and montmorillonite. — *Proc. Soil. Sci. Soc. Amer.* 16, 176—182.
- (40) GLAESER, R.: Complexes organo-argileux et rôle des cations échangeables. — These, Paris (1954).
- (41) GREENE-KELLEY, R.: Sorption of saturated organic compounds by montmorillonite. *Trans. Faraday Soc.* 52 (1956), 1281—1286.
- (42) BRINDLEY, G. W. & HOFMANN, R. W.: Orientation and packing of aliphatic chain molecules on montmorillonite. — *Clays and Clay Miner.* 9 (1952), 546—556.
- (43) BRINDLEY, G. W. & RAY, S.: Complexes of Ca-Montmorillonite with primary monohydric alcohols (Clay-organic studies-VIII). — *Amer. Miner.* 49 (1964), 106—115.
- (44) FISHER, L. F. & FISHER, M.: Advanced Organic Chemistry. — Reinhold Publishing Corporation, New York 1961.
- (45) JORDAN, J. W.: Organophilic bentonites. I. Swelling in organic liquids. — *J. Phys. and Colloid Chem.* 53 (1949), 294—306.
- (46) WEISS, A.; MEHLER, A. & HOFMANN, U.: Zur Kenntnis von organophilem Vermikulit. — *Z. Naturforsch.* 11b (1956), 431—434. Kationenaustausch und innerkristallines Quellvermögen bei den Mineralen der Glimmergruppe. — *Z. Naturforsch.* 11b (1956), 435—438.
- (47) BERGER, G.: The structure of Montmorillonite. — *Chem. Weekblad* 38 (1941), 42—43.
- (48) GIESEKING, J. E.: The Clay Minerals in Soils. — *Advances in Agronom.* 1 (1949), 59—204.
- (49) DIEHL, H.; HUBER, G. & IBERG, R.: Organische Derivate von Tonmineralien. — *Helv. chim. acta* 33 (1950), 1229—1232.
- (50) DIEHL, H.: Organische Derivate von Tonmineralien. — *Kolloid Z.* 124 (1951), 164—169.
- (51) MUKERJEE, H.: Synthetic Derivatives of Montmorillonit. — *Naturwiss.* 42 (1955), 412—413.
- (52) BROWN, G.; GREENE-KELLEY, R. & NORRISH, K.: Organic derivatives of montmorillonite. — *Clay Miner. Bull.* 1 (1952), 214—220.
- (53) GREENLAND, D. J. & RUSSELL, E. W.: Organo-clay derivatives and the origin of the negative charge on clay particles. — *Trans. Faraday Soc.* 51 (1955), 1300—1307.
- (54) SCHWARZ, R. & HENNIGKE, H. W.: Silicic acids, XIII. Crystalline disilicic acid and its suitability as a type substance. — *Z. anorgan. Chem.* 283 (1956), 346—350.
- (55) VAN OLPHEN, H. & DEEDS, C. T.: Stepwise hydration of clay-organic complexes. — *Nature* 194 (1962), 176—177.


Table I

Substances showing interlamellar sorption

Substance	Charge on Layer	Complexing Substances	Investigator(s)
(1) <i>Clay Minerals</i>			
Montmorillonite, etc.	-	Cations, neutral molecules	Numerous
Vermiculite	-	Cations, neutral molecules	Barshad, Walker, etc.
Halloysite	0 or \pm	Neutral molecules, salts	MacEwan; Henin, etc.; Walker
(2) <i>Other Minerals</i>			
Micas	-	Cations, neutral molecules (?)	Hofmann, etc.
U-micas, etc.	-	Cations, neutral molecules	Hofmann, etc.
Tobermorite etc.	?	?	
(3) <i>Chemical Precipitates, etc.</i>			
Graphitic acid	-	Cations, neutral molecules	Hofmann, etc.; MacEwan, etc.
Gypsum (ppt.)	?	Neutral molecules (?)	Cano and MacEwan
Complex cyanides of Fe^{3+} , Co^{3+} , etc.	0	Neutral molecules	Weiss
α -hydroxides of Zn^{2+} , etc.	+	Anionic dyestuffs, neutral molecules	Talibudeen, etc.

Table II

The basal spacings of alcohol - C_4AH_x complexes

Alcohol	Formula	Basal spacing (Å)	Difference (Å)
Methanol*	$\text{CH}_3 \cdot \text{OH}$	12,90	----- 2,8
ethanol	$\text{CH}_3 \cdot \text{CH}_2 \cdot \text{OH}$	15,72	----- 1,7
n-propyl alcohol	$\text{CH}_3 \cdot (\text{CH}_2)_2 \cdot \text{OH}$	17,40	----- 2,8
n-butyl alcohol	$\text{CH}_3 \cdot (\text{CH}_2)_3 \cdot \text{OH}$	20,20	----- 1,8
n-amyl alcohol	$\text{CH}_3 \cdot (\text{CH}_2)_4 \cdot \text{OH}$	22,00	----- 2,7
n-hexyl alcohol	$\text{CH}_3 \cdot (\text{CH}_2)_5 \cdot \text{OH}$	24,66	----- 1,8
n-heptyl alcohol	$\text{CH}_3 \cdot (\text{CH}_2)_6 \cdot \text{OH}$	26,56	----- 2,7
n-octyl alcohol	$\text{CH}_3 \cdot (\text{CH}_2)_7 \cdot \text{OH}$	29,28	----- 2,5
n-nonyl alcohol	$\text{CH}_3 \cdot (\text{CH}_2)_8 \cdot \text{OH}$	31,77	----- 4,4
n-decyl alcohol**)	$\text{CH}_3 \cdot (\text{CH}_2)_9 \cdot \text{OH}$	36,19	
benzyl alcohol	 $\cdot (\text{CH}_2) \cdot \text{OH}$	20,60	
i-propyl alcohol	$\text{CH}_3 \cdot \text{CH} \cdot \text{OH}$ CH_3	10,68	
i-amyl alcohol	$\text{CH}_3 \cdot \text{CH} \cdot (\text{CH}_2)_3 \cdot \text{OH}$ CH_3	10,6 > 20,8	

*) Other methanol/ C_4AH_x complexes: $d_{001} = 14.4$; 13.8 and 10.8 Å.

**) Alcohols C_{11} to C_{20} are no longer subject to interlamellar sorption in solutions with ether or acetone

Table III

Intra- and intermolecular spacing

Intramolecular:

$$r_O = 1.40 \text{ \AA}; r_H = 1.20 \text{ \AA}$$

C - C	= 1.54 $\overset{\circ}{\text{\AA}}$	all bond angles are 109.5° angle of inclination of carbon chain $\sim 67^\circ$
C - O	= 1.43 $\overset{\circ}{\text{\AA}}$	
C - H	= 1.08 $\overset{\circ}{\text{\AA}}$	

Changes of basal spacing of the complex:

Intermolecular:

$H_3C \dots CH_3 = 3.5 \overset{\circ}{\text{\AA}}$	from C_{even} to $C_{\text{odd}} = 1.7, \overset{\circ}{\text{\AA}}$	} cf. Table II
$O - H \dots O = 2.6 \overset{\circ}{\text{\AA}}$	from C_{odd} to $C_{\text{even}} = 2.75 \overset{\circ}{\text{\AA}}$	

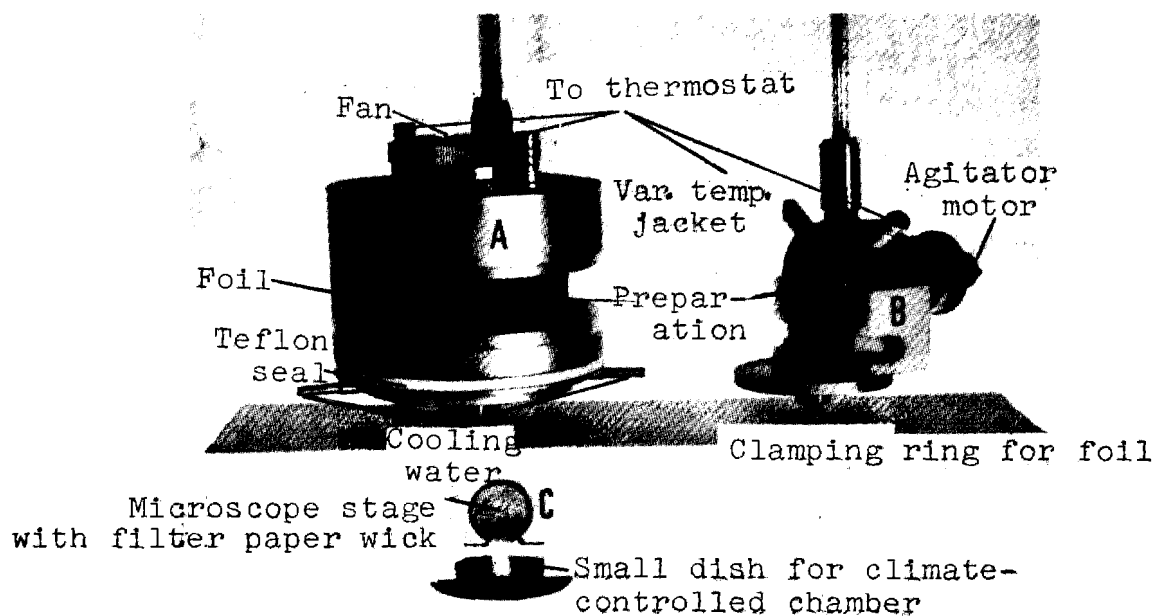


Fig. 1

- A. Climate-controlled x-ray chamber
- B. X-ray chamber for suspensions
- C. Arrangement of "wick preparation support" for the climate controlled chamber

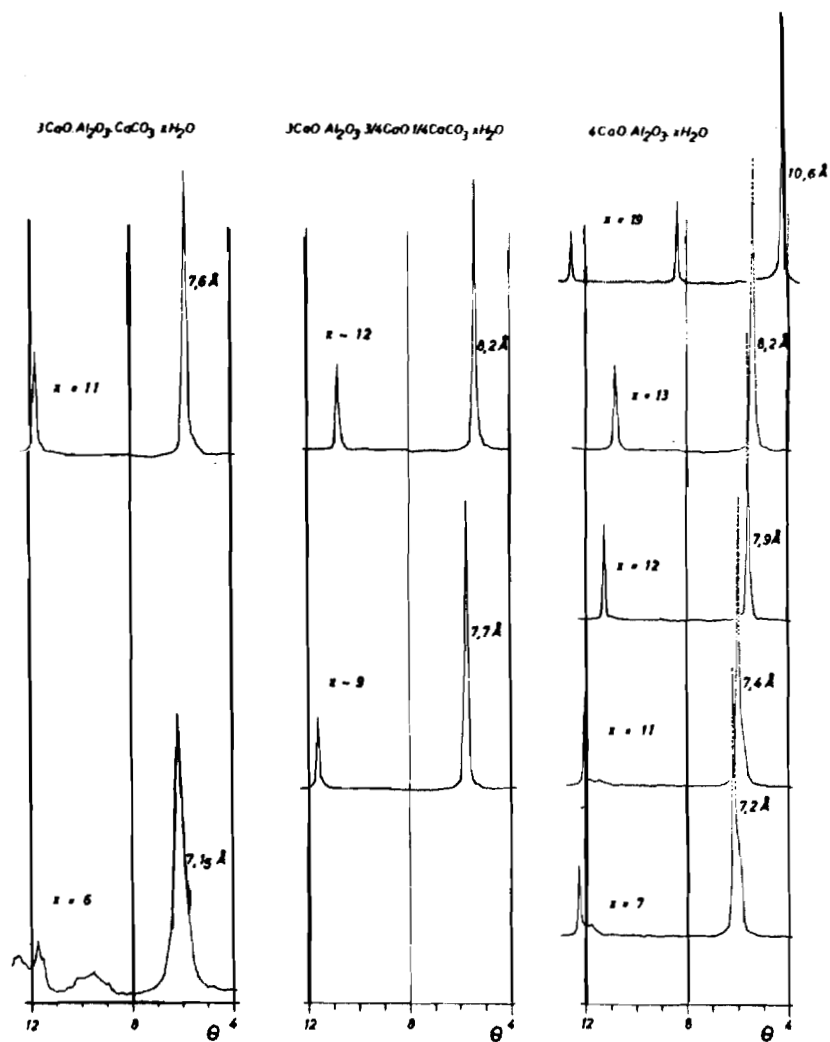


Fig. 2

Tetracalcium aluminate hydrate and tetracalcium aluminate carbonate hydrate, after⁽²¹⁾

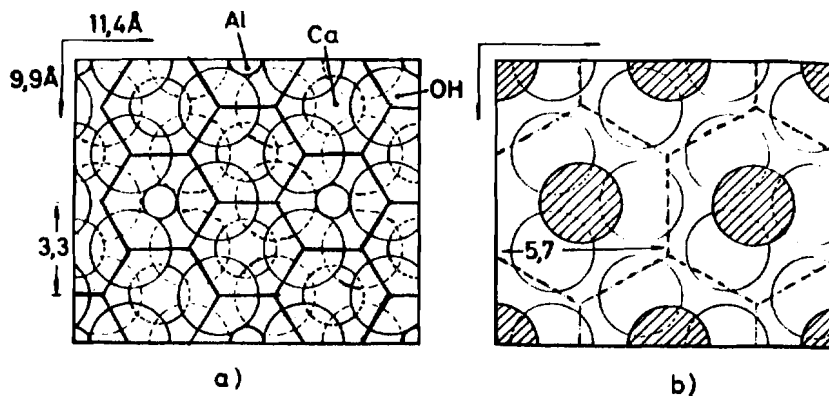


Fig. 3

- (a) Octahedron sheet $\text{Ca}_2\text{Al}(\text{OH})_6$;
 (b) "Outer OH" (hatched), ordered,
 or distributed statistically
 over both sides of the octahedron
 sheet

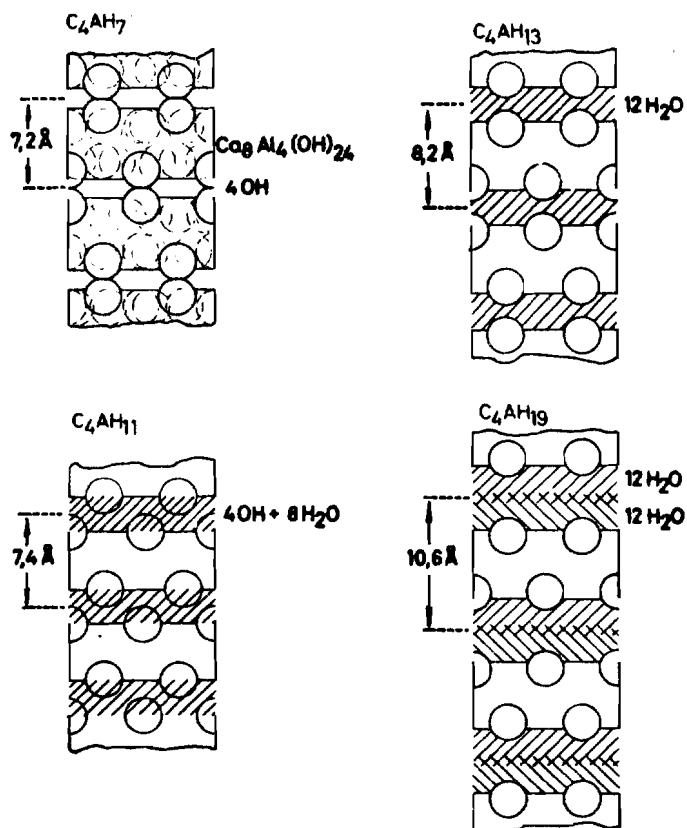


Fig. 4

Possible configuration of hydrate stages of C_4AH_x

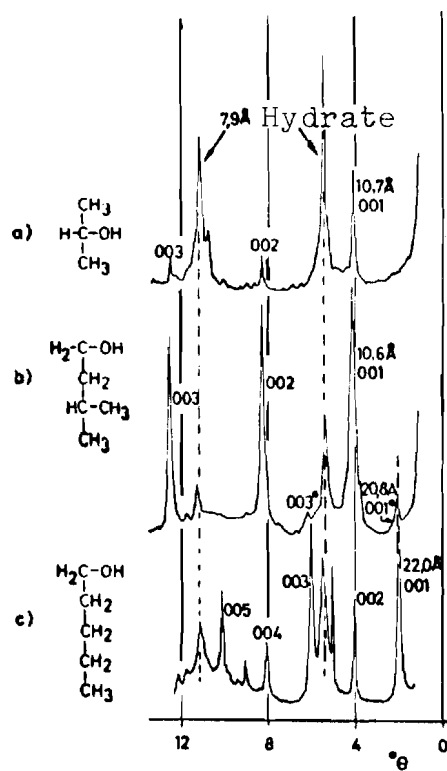


Fig. 5

C_4AH_x complexes with i-propanol (a),
i-amyl alcohol (b), and n-amyl alcohol (c).
Unconverted TCAH with 7.9 Å

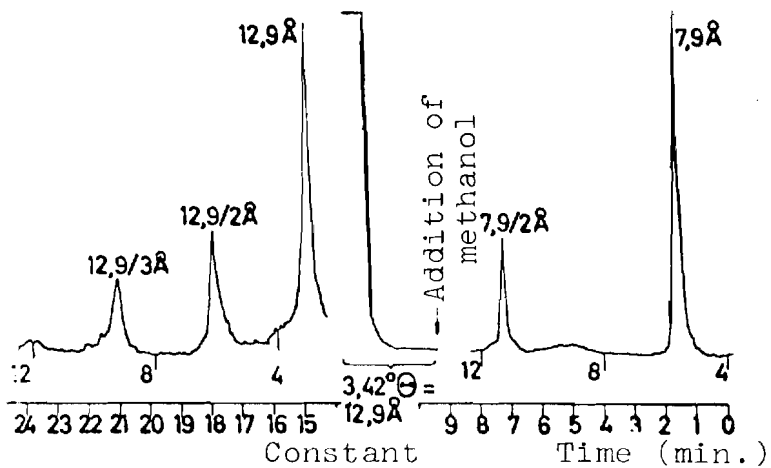


Fig. 6

Rate of sorption of methanol in TCAH

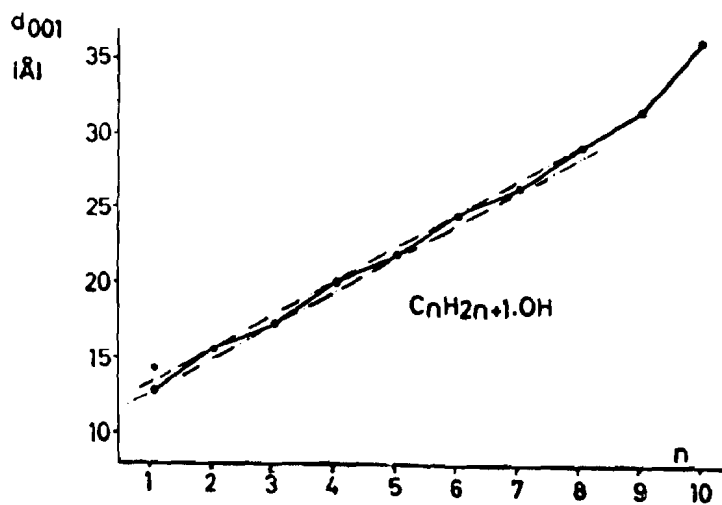


Fig. 7

C_4AH_x complexes of n-alcohols

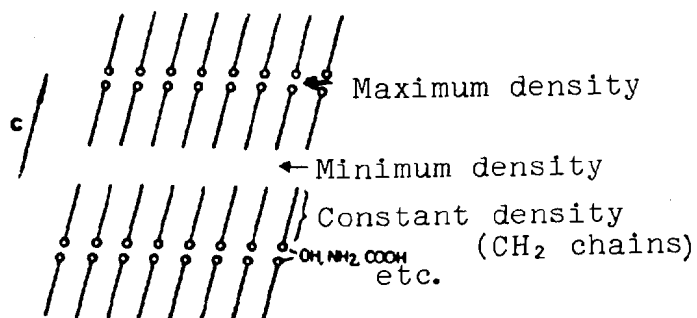


Fig. 8

Density distribution in crystalline fatty acids, alcohols, amines, etc.

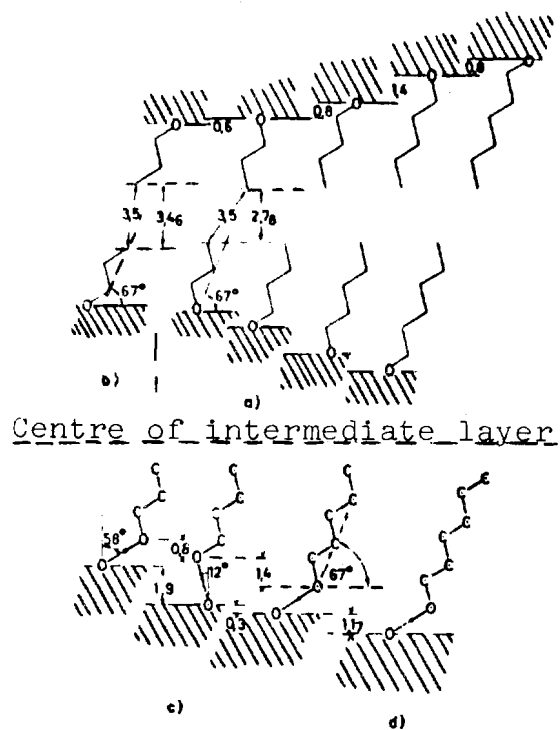


Fig. 9

Alcohol molecules between C_4AH_x layers (hatched).
 a,b: bonds not taken into account;
 c,d: models for H binding

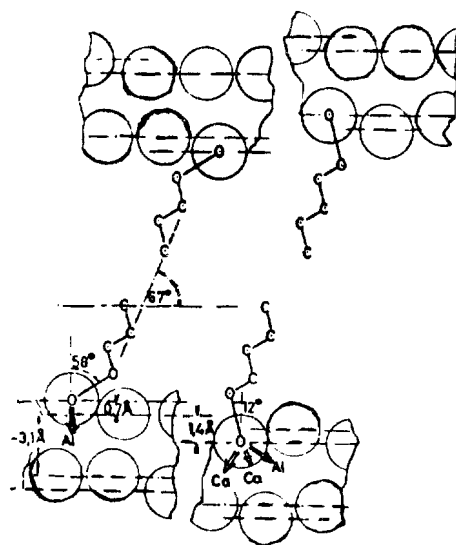


Fig. 10

H binding of alcohol complexes; alcohols with C_{even} to octrahedral OH, with C_{odd} to the outer OH of the TCAH layer

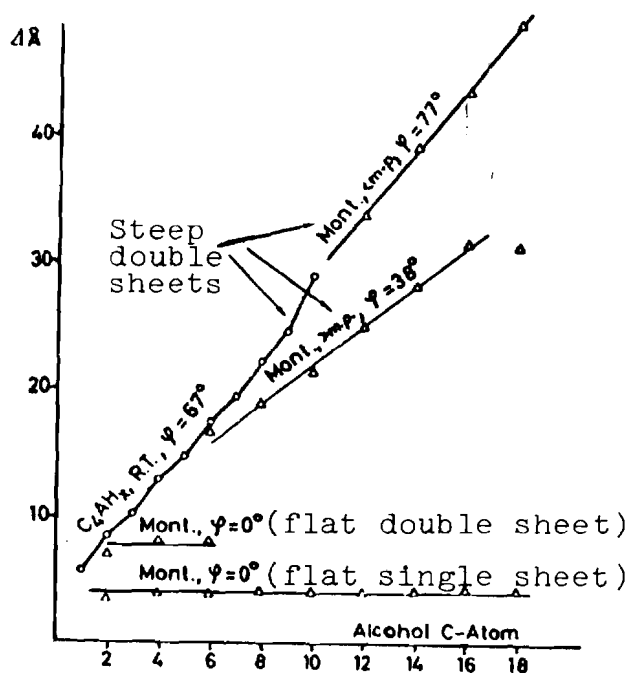


Fig. 11

Comparison of alcohol complexes of C_4AH_x (circles)
and Ca montmorillonite⁽⁴³⁾ (triangles).

Effective divergence ΔA of sheets by the alcohol molecules,

ΔA = basal spacing of inorganic substance

(7.2 Å for C_4AH_x , cf. Figure 2 or 9.7 Å for Ca montmorillonite⁽⁴³⁾).

θ = angle of inclination of the alcohol molecules

m.p. = melting point of the alcohols

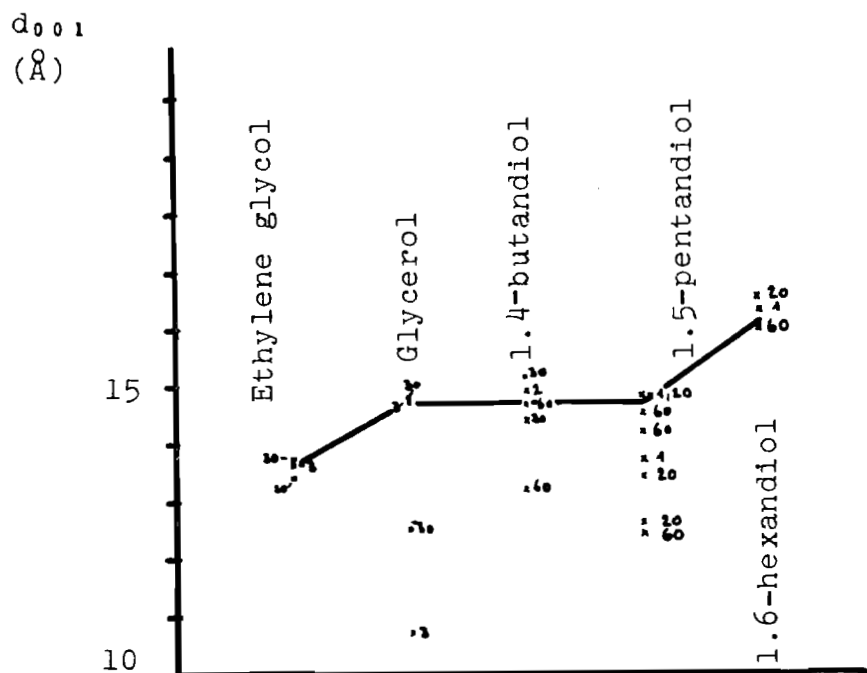


Fig. 12

C_4AH_x complexes of multivalent alcohols

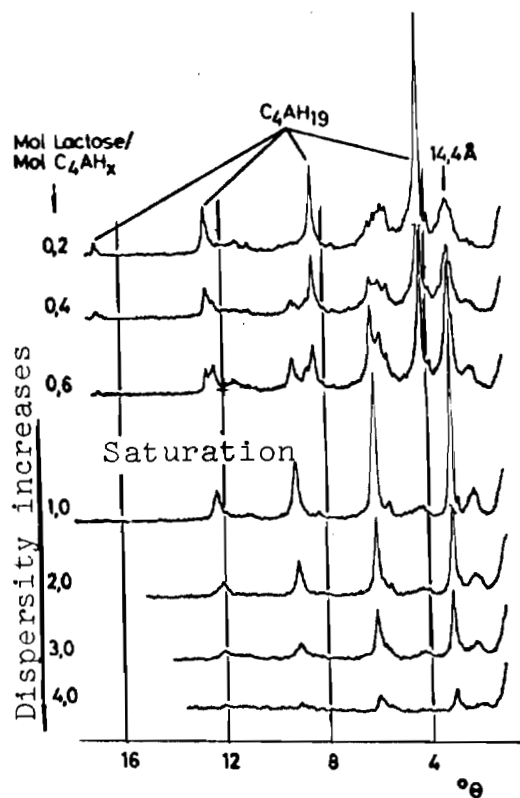


Fig. 13

Reaction of C_4AH_x with lactose in water

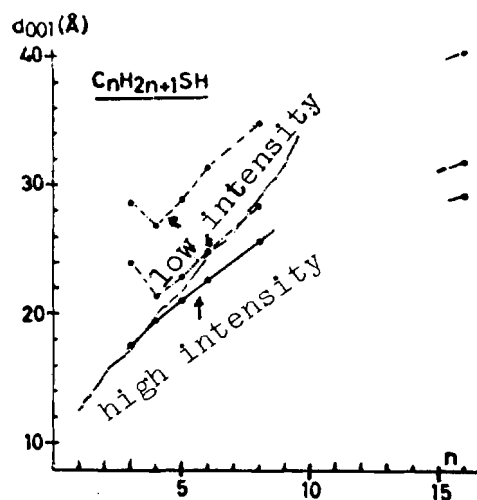


Fig. 14

C_4AH_x complexes of mercaptan

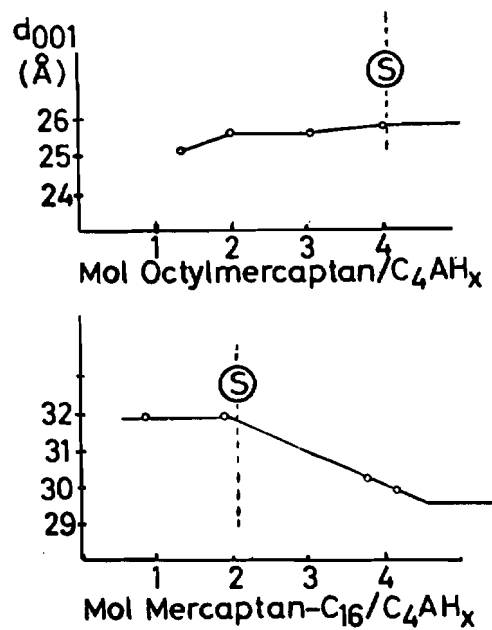


Fig. 15

Sorption capacity of C_4AH_x for octyl and hexadecyl mercaptan. (S)^x = saturation

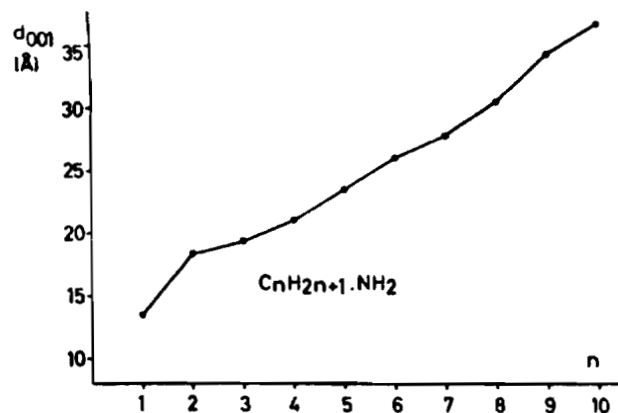


Fig. 16

C_4AH_x complexes of n-amines

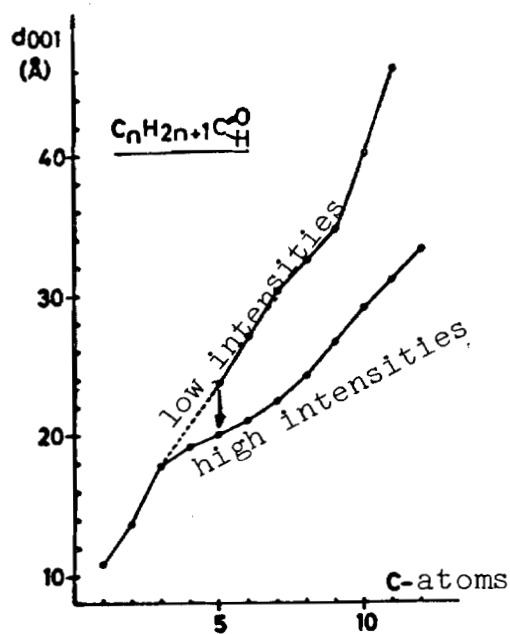


Fig. 17

C_4AH_x complexes of aldehydes

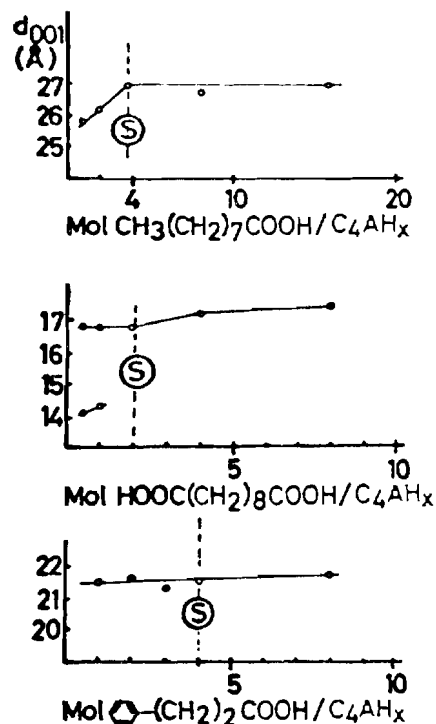


Fig. 18

Sorption capacity of C₄AH_x for undecanoic acid, sebacic acid and β-phenyl propionic acid.

Ⓢ = saturation

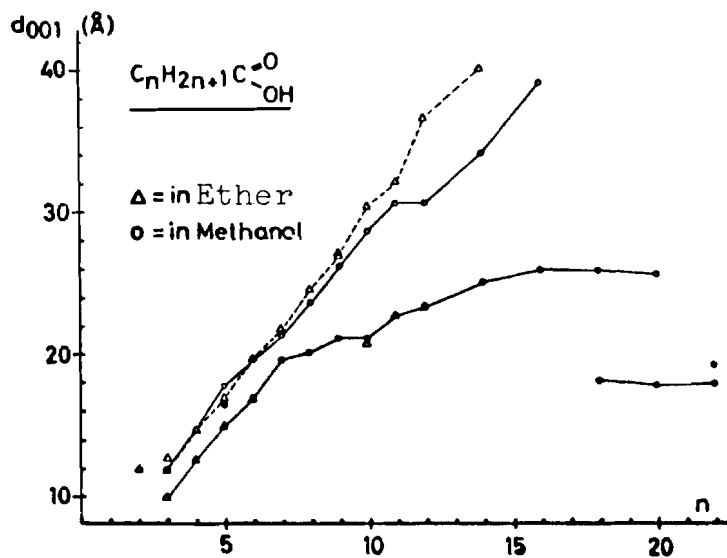


Fig. 19

C₄AH_x complexes of the fatty acids

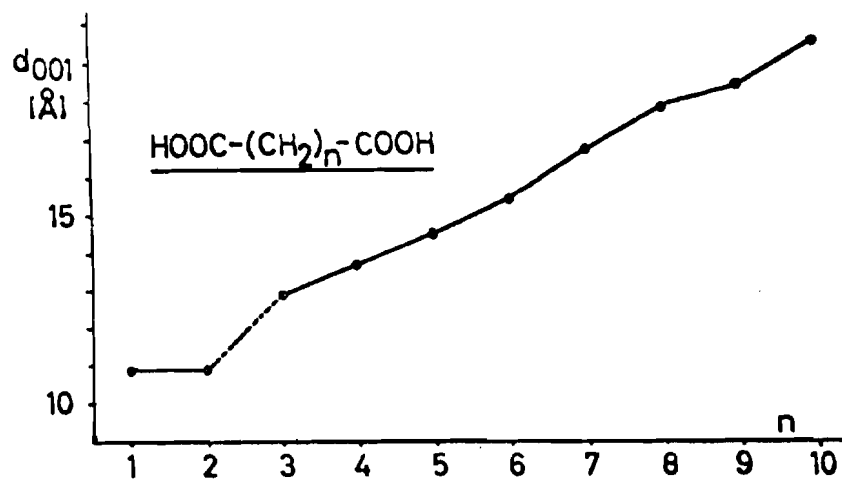


Fig. 20

C₄AH_x complexes of the α,ω dicarboxylic acids

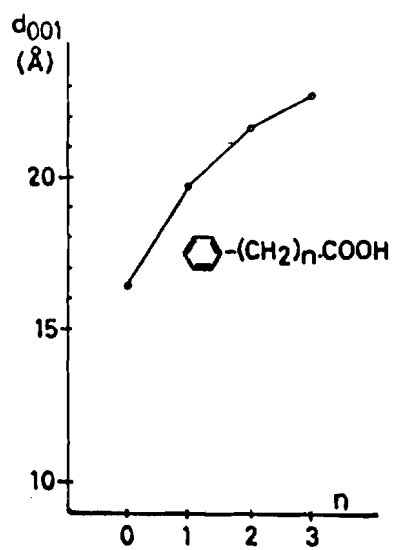


Fig. 21

C₄AH_x complexes of the phenyl carboxylic acids

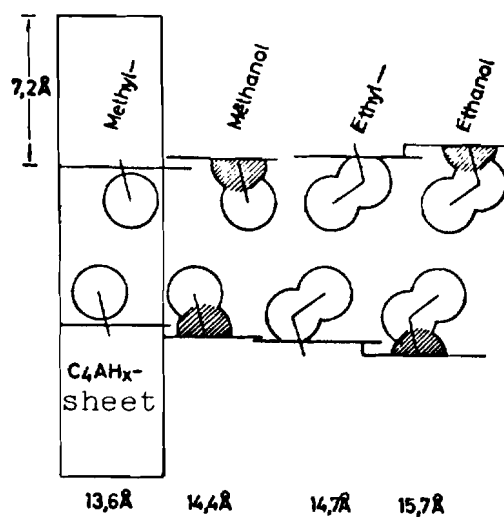


Fig. 22

Arrangement of molecules in methylated and ethylated C_4AH_x compared with the methanol and ethanol complexes of C_4AH_x

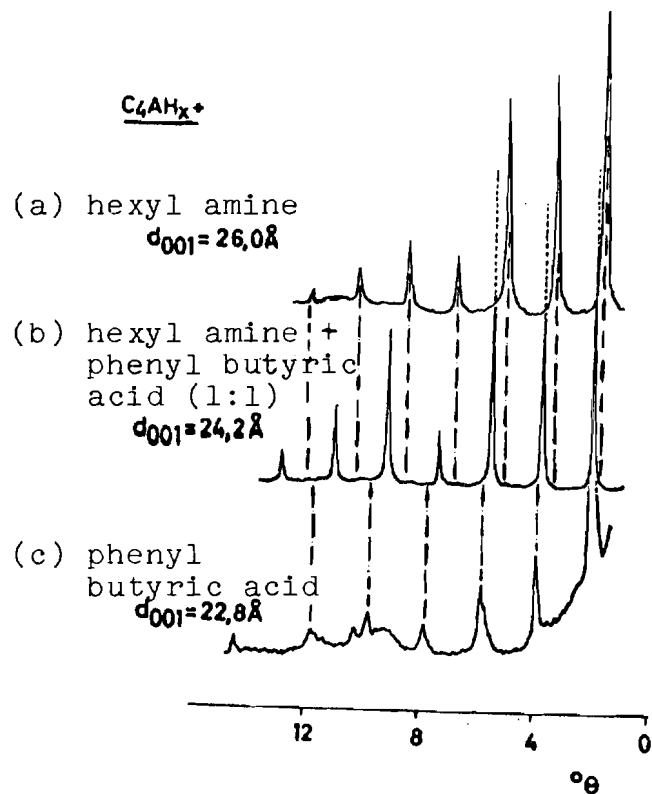


Fig. 23

Sorption of an amine (a), a carboxylic acid (c) and a 1:1 mixture of both (b) in C_4AH_x

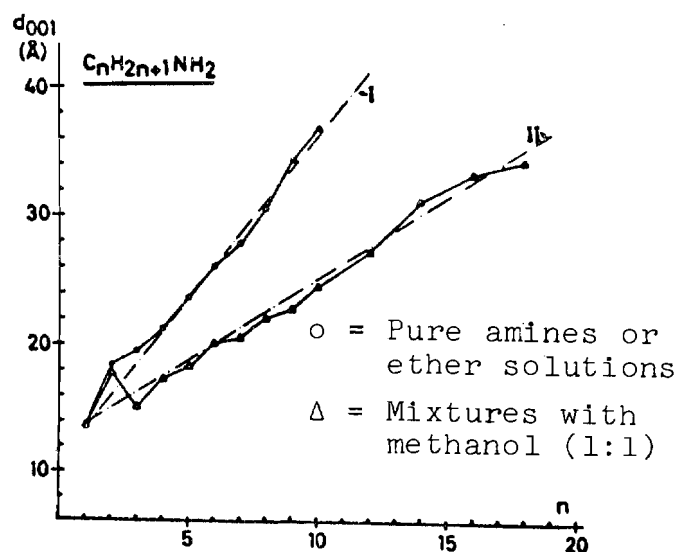


Fig. 24

Sorption of amines mixed with methanol in C_4AH_x (triangles) compared with complexes with amines alone (circles)

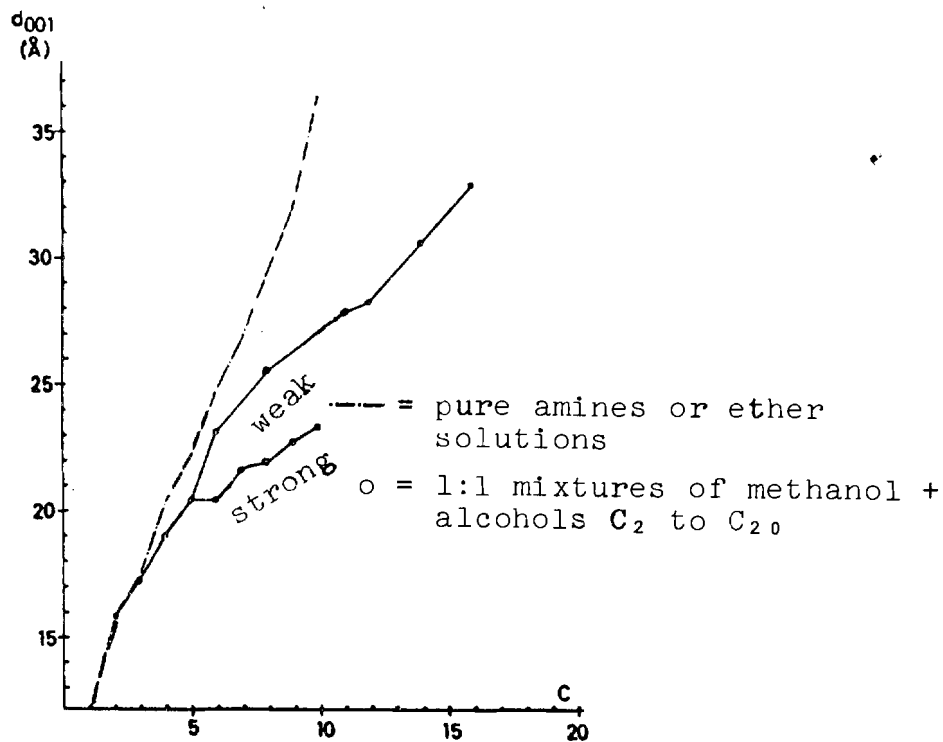


Fig. 25

Sorption of long-chain alcohols mixed with methanol in C_4AH_x compared with the complexes of unmixed alcohols (dashed line)

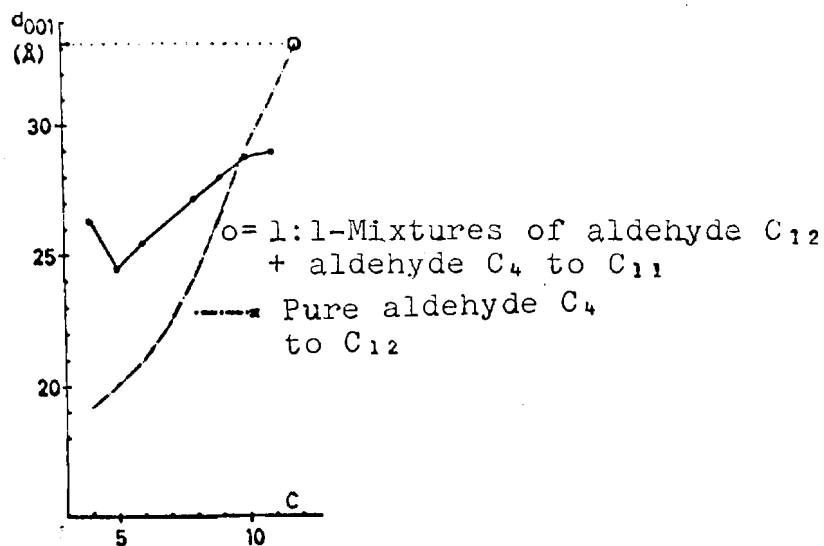
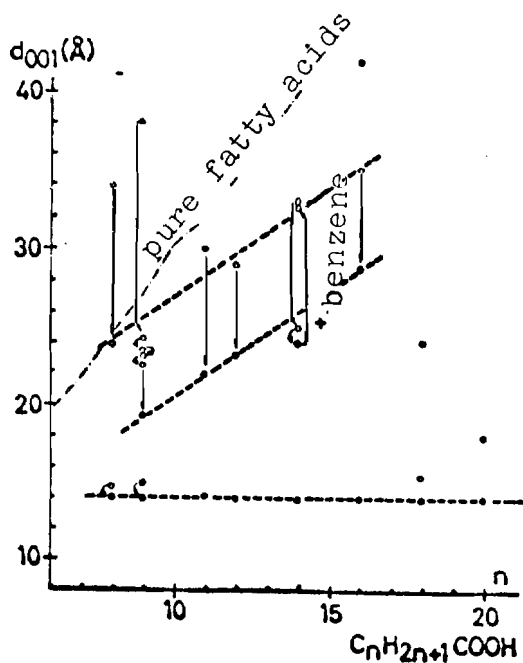


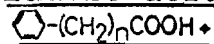
Fig. 26

Sorption of a long-chain aldehyde mixed with various short-chain aldehydes, compared with the C_4AH_x complexes of unmixed aldehydes (dashed curve)

Benzoic acid + $C_nH_{2n+1}COOH$ + Benzene



Lauric acid +



benzene

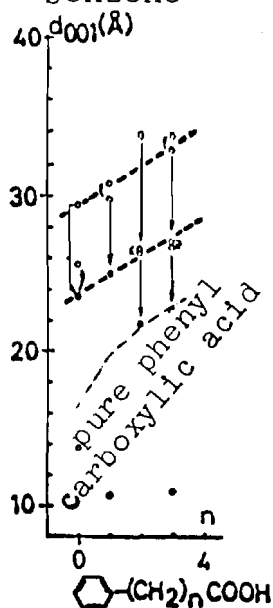


Fig. 27

Sorption of a mixture of three organic substances in C_4AH_x

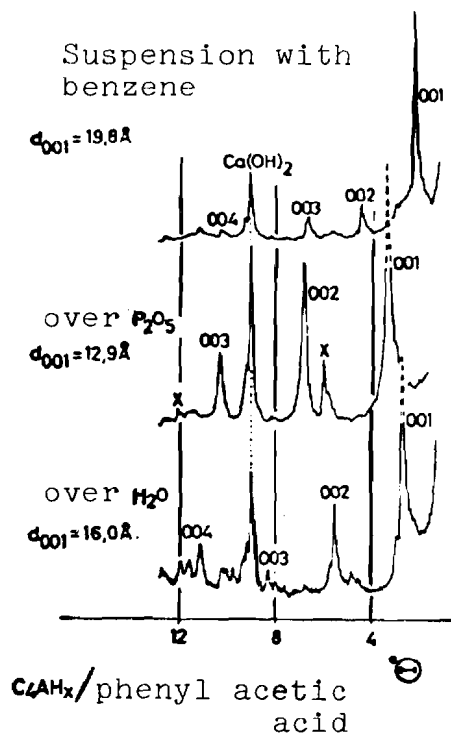


Fig. 28

Phenyl acetic acid complex of C_4AH_x
under different conditions
of vapour pressure

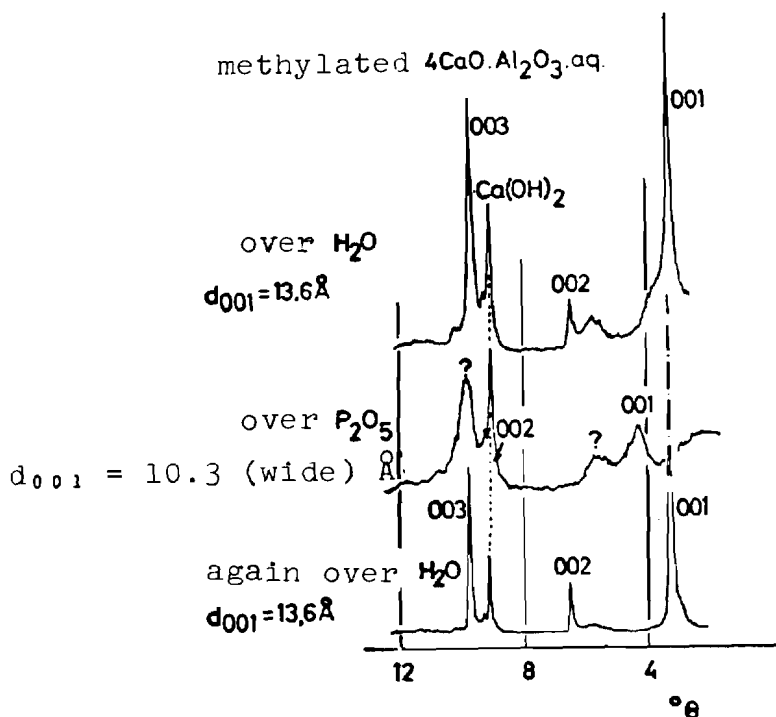


Fig. 29

Methylated C_4AH_x between 0 and 100% relative humidity

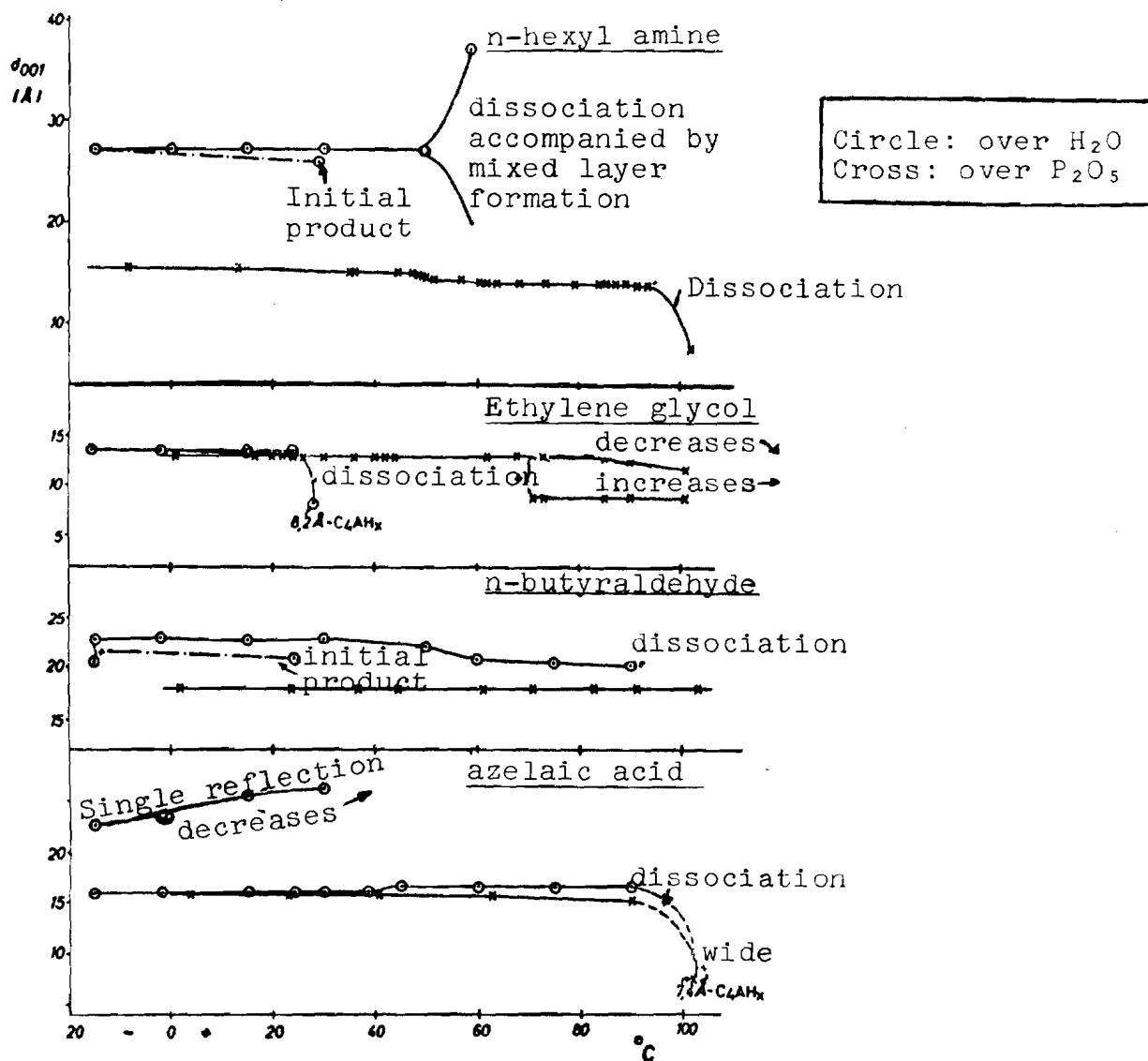


Fig. 30

Treatment of the C_4AH_x complex of n-hexyl amine, ethylene glycol, n-butyraldehyde and azelaic acid at 0 and 100% relative humidity in the temperature range of -20 to 100°C